

2

ITC FILE 001

AD-A192 315

STOCHASTIC GEOLOGIC EFFECTS  
ON NEAR-FIELD GROUND MOTIONS  
IN ALLUVIUM

R. E. Reinke  
B. W. Stump

November 1987

Final Report

DTIC  
ELECTE  
MAR 22 1988  
S D  
CH

Approved for public release; distribution unlimited.

AIR FORCE WEAPONS LABORATORY  
Air Force Systems Command  
Kirtland Air Force Base, NM 87117-6008

88 3 21 020

This final report was prepared by the Air Force Weapons Laboratory, Kirtland Air Force Base, New Mexico under Job Order 88091392. Dr Robert E. Reinke (NTES) was the Laboratory Project Officer-in-Charge.

When Government drawings, specifications, or other data are used for any purpose other than in connection with a definitely Government-related procurement, the United States Government incurs no responsibility or any obligation whatsoever. The fact that the Government may have formulated or in any way supplied the said drawings, specifications, or other data, is not to be regarded by implication, or otherwise in any manner construed, as licensing the holder, or any other person or corporation; or as conveying any rights or permission to manufacture, use, or sell any patented invention that may in any way be related thereto.

This report has been authored by employees of the United States Government. Accordingly, the United States Government retains a nonexclusive, royalty-free license to publish or otherwise reproduce the material contained herein, or allow others to do so, for United States Government purposes.

This report has been reviewed by the Public Affairs Office and is releasable to the National Technical Information Service (NTIS). At NTIS, it will be available to the general public, including foreign nations.

If your address has changed, if you wish to be removed from our mailing list, or if your organization no longer employs the addressee, please notify AFWL/NTES, Kirtland AFB, NM 87117-6008 to help us maintain a current mailing list.

This technical report has been reviewed and is approved for publication.

ROBERT E. REINKE, PhD  
Project Officer

*Robert E Reinke*

*Thomas E Bretz*  
THOMAS E. BRETZ, JR  
Lt Col, USAF  
Chief, Applications Branch

FOR THE COMMANDER

*Carl L Davidson*  
CARL L. DAVIDSON  
Colonel, USAF  
Chief, Civil Engrg Research Division

DO NOT RETURN COPIES OF THIS REPORT UNLESS CONTRACTUAL OBLIGATIONS OR NOTICE ON A SPECIFIC DOCUMENT REQUIRES THAT IT BE RETURNED.

# REPORT DOCUMENTATION PAGE

1a. REPORT SECURITY CLASSIFICATION <b>UNCLASSIFIED</b>		1b. RESTRICTIVE MARKINGS	
2a. SECURITY CLASSIFICATION AUTHORITY		3. DISTRIBUTION / AVAILABILITY OF REPORT  Approved for public release; distribution unlimited.	
2b. DECLASSIFICATION / DOWNGRADING SCHEDULE			
4. PERFORMING ORGANIZATION REPORT NUMBER(S)  AFWL-TR-86-133		5. MONITORING ORGANIZATION REPORT NUMBER(S)	
6a. NAME OF PERFORMING ORGANIZATION  Air Force Weapons Laboratory	6b. OFFICE SYMBOL (if applicable) NTES	7a. NAME OF MONITORING ORGANIZATION	
6c. ADDRESS (City, State, and ZIP Code)  Kirtland Air Force Base, NM 87117-6008		7b. ADDRESS (City, State, and ZIP Code)	
8a. NAME OF FUNDING / SPONSORING ORGANIZATION	8b. OFFICE SYMBOL (if applicable)	9. PROCUREMENT INSTRUMENT IDENTIFICATION NUMBER	
8c. ADDRESS (City, State, and ZIP Code)		10. SOURCE OF FUNDING NUMBERS	
		PROGRAM ELEMENT NO. 62601F	PROJECT NO. 8809
		TASK NO. 13	WORK UNIT ACCESSION NO. 92
11. TITLE (Include Security Classification)  STOCHASTIC GEOLOGIC EFFECTS ON NEAR-FIELD GROUND MOTIONS IN ALLUVIUM			
12. PERSONAL AUTHOR(S) Reinke, Dr R.E.; and Stump, B.W.			
13a. TYPE OF REPORT Final	13b. TIME COVERED FROM 1 Jan 84 TO 30 Jun 86	14. DATE OF REPORT (Year, Month, Day) 1987 November	15. PAGE COUNT 50
16. SUPPLEMENTARY NOTATION			
17. COSATI CODES		18. SUBJECT TERMS (Continue on reverse if necessary and identify by block number)	
FIELD 08	GROUP 11	Ground motion      Ground motion simulation      Spectral High explosive      Stochastic characterization      analysis Explosive arrays      Geologic inhomogeneity	
19. ABSTRACT (Continue on reverse if necessary and identify by block number) Analysis of accelerograms recorded at the 20-m range from a buried 5-lb detonation in alluvium revealed wide (as large as 20 dB in the amplitude modulus of the Fourier transform) variations in response for frequencies above 35 Hz. Additional experiments were performed which ruled out source asymmetry or instrumental irregularity as the cause of these variations. The observations suggest that scattering by geologic inhomogeneity is responsible for the frequency-dependent spatial variability in ground motion. A thorough understanding of the physical processes responsible for this variability requires that a quantitative relationship be established between the subsurface material property information and the observed ground motion characteristics. An attempt was made to do this using available standard penetration test (SPT) data from the test-bed where the initial experiment was detonated. Autocorrelations of the blow count data from the SPT test were computed and compared with theoretical exponential and Gaussian distributions. The exponential distribution with a scale length between 2.0 and 3.0 m best matches the data. Assuming the (over)			
20. DISTRIBUTION / AVAILABILITY OF ABSTRACT <input checked="" type="checkbox"/> UNCLASSIFIED/UNLIMITED <input type="checkbox"/> SAME AS RPT <input type="checkbox"/> DTIC USERS		21. ABSTRACT SECURITY CLASSIFICATION UNCLASSIFIED	
22a. NAME OF RESPONSIBLE INDIVIDUAL Reinke, Dr Robert E.		22b. TELEPHONE (Include Area Code) (505) 844-0484	22c. OFFICE SYMBOL NTES

## 19. ABSTRACT (Continued)

Born approximation, a scale length of 2.0 to 3.0 m implies that significant scattering should occur above 10 Hz. The recorded ground motions are, however, coherent out to about 35 Hz, suggesting a scale length of 0.5 to 1.0 m, which is beyond the resolution of the SPT technique. This scale length is not unreasonable in light of the general geologic characteristics of the test area.

## CONTENTS

	<u>Page</u>
INTRODUCTION	1
THE INITIAL EXPERIMENT--THE ART 2 TEST	3
EXPERIMENTAL DESIGN	9
STOCHASTIC/DETERMINISTIC CLASSIFICATION TOOLS AND DATA ANALYSIS	14
NEW SITE CHARACTERIZATION PROCEDURE	23
RELATION OF OBSERVED AZIMUTHAL VARIABILITY TO TEST SITE GEOLOGY	30
DISCUSSION AND CONCLUSIONS	39
REFERENCES	41



<b>Accession For</b>	
NTIS GRA&I	<input checked="" type="checkbox"/>
DTIC TAB	<input type="checkbox"/>
Unannounced	<input type="checkbox"/>
Justification	
By	
Distribution/	
<b>Availability Codes</b>	
Dist	Avail and/or Special
A-1	

## FIGURES

<u>Figure</u>		<u>Page</u>
1.	Experimental layout for the ART 2 Test Event.	5
2.	Filtered vertical acceleration records from ART 2.	6
3.	Filtered radial acceleration records from ART 2.	7
4.	Vertical and radial Fourier acceleration spectra for ART 2.	8
5.	Experimental layout for Huddle Test.	10
6.	Vertical and radial Fourier acceleration spectra from Huddle Test.	11
7.	Test-bed layout for the ART II tests.	12
8.	Computed coherencies for ART 2.	15
9.	Mean and variance of ART 2 spectral ensembles.	16
10.	Spectral coefficient of variation curves for the ART II pit shots compared with ART 2.	18
11.	Spectral coefficient of variation curves for the vertical and radial components of the Huddle Test.	19
12.	Comparison of vertical acceleration spectra for the five shots of the ART II series.	20
13.	Comparison of 10-m and 30-m coefficient of variation curves for ART III 2.	22
14.	Mean and variance of spectra for four shots of the Seisgun at the same site.	24
15.	Comparison of Seisgun Huddle Test coefficient of variation with full circle array coefficient of variation.	26
16.	Comparison of the coefficient of variation curves for three Seisgun shots at the ART III-2 site and one shot at Site A.	27
17.	Comparison of 20-m and 30-m coefficient of variation curves for the Seisgun.	29
18.	Generalized geologic cross section of McCormick Ranch.	31
19.	Layout of boreholes within the ART 2 test-bed and isopach map of blow counts.	32

## FIGURES (Concluded)

<u>Figure</u>		<u>Page</u>
20.	Plots of blow counts vs depth (data points from all 18 boreholes are included) .	33
21.	Experimental autocorrelation function compared with Gaussian and exponential autocorrelation functions. (The lines on the plot are the theoretical autocorrelation functions; the experimental autocorrelation functions from all holes are represented by data points.)	36
22.	Plot of scattered energy as a function of frequency for different scale lengths.	37

## INTRODUCTION

Several recent studies have found a lack of coherence between ground motion waveforms recorded at stations separated by only a few tens of meters. Reference 1 covers the station-to-station waveform coherence for near-field explosion accelerograms recorded on a nine-station array at Pahute Mesa, Nevada Test Site. For this array, at a range of 6 km from a 5.6 M<sub>L</sub> underground explosion with an interstation spacing of 100 meters, strong incoherent signals were found above 5 Hz on all components. This incoherence was attributed to scattering. Reference 2 discusses earthquake seismogram coherence for a nine-station array with an interstation spacing of 50 m. This temporary array was located near the Pinon Flat Observatory in California. Several events with magnitudes between 3.0 and 4.2 and hypocentral distances ranging from 10 to 50 km were analyzed. For this data set, P waves were found to be coherent up to the 25 to 30-Hz region, and S waves up to about 15 Hz. This variability in ground motion over such short distances raises questions about the appropriateness of using single station point measurements of the ground motion field for the inversion of source functions as well as the use of the peak ground acceleration (PGA) statistic based on single-point measurements.

Reference 3 analyses the near-field motions from the 1979 Imperial Valley Earthquake. This data set was obtained from a closely spaced array of five stations. This study confirmed that incoherence of higher frequency ground motions could, because of averaging effects, reduce the high-frequency input to buildings with foundations of large areal extent. Analysis of this particular data set suggested that base averaging reduction factors of 10 to 30 percent would have occurred for foundations 50 m in diameter for frequencies above 20 Hz. No significant reduction would have occurred for frequencies below 5 Hz.

This frequency-dependent spatial variability in ground motion has also been observed on some small-scale, high-explosive tests conducted in dry alluvium (Ref. 4). An array of six triaxial accelerometers spaced at six azimuths at the 20-m range from a buried 5-lb\* detonation yielded waveforms

\*To convert from lb to kg, multiply by 4.535924 E-01.



which were incoherent above 30 to 35 Hz. In an effort to determine whether these variations were induced by instrumentation, source asymmetry or scattering due to geologic variability, a series of small-scale, high-explosive experiments were performed. This paper describes the results of these experiments, an effort to develop a simple seismic survey technique which could be used to determine the coherence function of the geological structure at a given test site, and the physical interpretation of the data.

## THE INITIAL EXPERIMENT--THE ART 2 TEST

The Array Test Series (ARTS) was a series of single and multiple 5-lb explosive tests conducted in dry alluvium. The ARTS was formulated, designed and implemented to investigate the quantitative effects of finite explosive sources upon observed motion fields. The single-burst tests in the series were intended to thoroughly characterize the single-burst ground motion environment (Ref. 5). One of these tests, ART 2 (Table 1), was intended to determine the degree of azimuthal variation in ground motion levels resulting from a single charge event. The experimental layout for this test is shown in Fig. 1. Six triaxial servo accelerometers were placed at the 20-m range at six different azimuths. These accelerometers were recorded by 3-channel digital event recorders at a rate of 200 samples/second with a 5-pole low-pass Butterworth filter at 70 Hz. The original accelerograms, along with low-pass (30-Hz corner) and high-pass (40-Hz corner) filtered versions, are shown in Figs. 2 and 3. Fourier acceleration spectra for the waveforms are shown in Fig. 4. Examination of the acceleration traces and the spectra in these figures reveals considerable similarity in the various waveforms below 30 Hz, while large azimuthal amplitude variations are observed for frequencies above 30 to 35 Hz. The accelerograms show that the high-frequency energy arrives after the initial coherent low-frequency response, with a great variability in wave shape as well as amplitude. The vertical and radial spectral shapes (Fig. 4) are similar between 5 and 35 Hz; above 35 Hz, variations up to 15-20 dB occur.

TABLE 1. Description of experiments.

Experiment	Description
ART 1	Single 5-lb charge buried at 1 m. Recording array - 6 triaxial accelerometers at different azimuths at the 20-m range.
ART 19	"Huddle Test." Single 5-lb charge buried at 1 m recorded by 6 triaxial accelerometers in a closely spaced group at the 20-m range.
ART II	The "Pit Shots." Series of five 5-lb buried charges all fired at the same ground zero and recorded by 6 triaxial accelerometers spaced at equal azimuths at the 20-m range. The initial charge was detonated in situ; subsequent charges were fired in a sand-filled pit.
ART III-2	Single 5-lb buried charge recorded by 6 accelerometers at the 10-m range and 6 accelerometers at the 30-m range. Accelerometers spaced at equal azimuths.
Shotgun Tests	Seisgun recorded by 12 or 24 vertical geophones at ranges from 10 to 30 m.

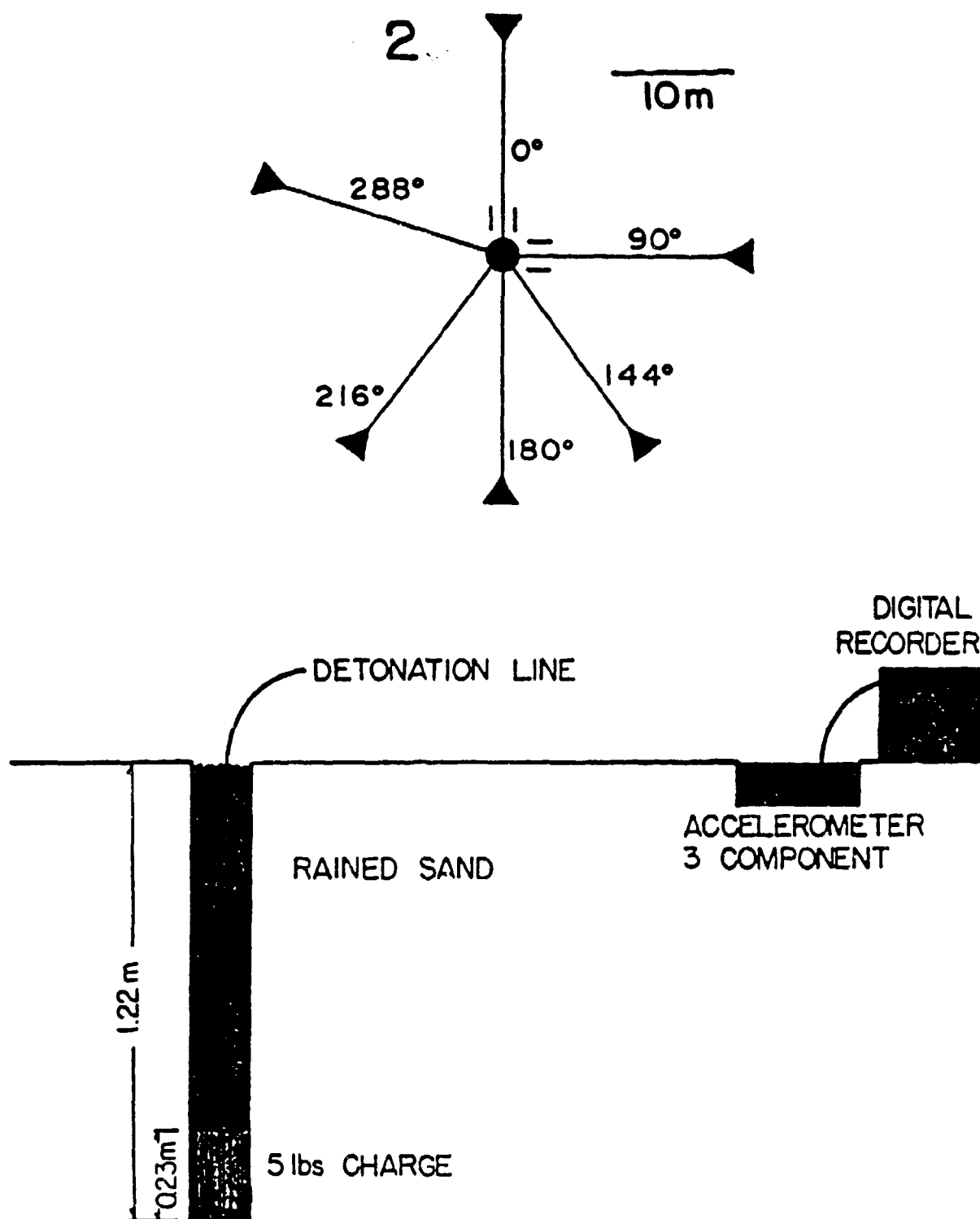


Figure 1. Experimental layout for the ART 2 Test Event.

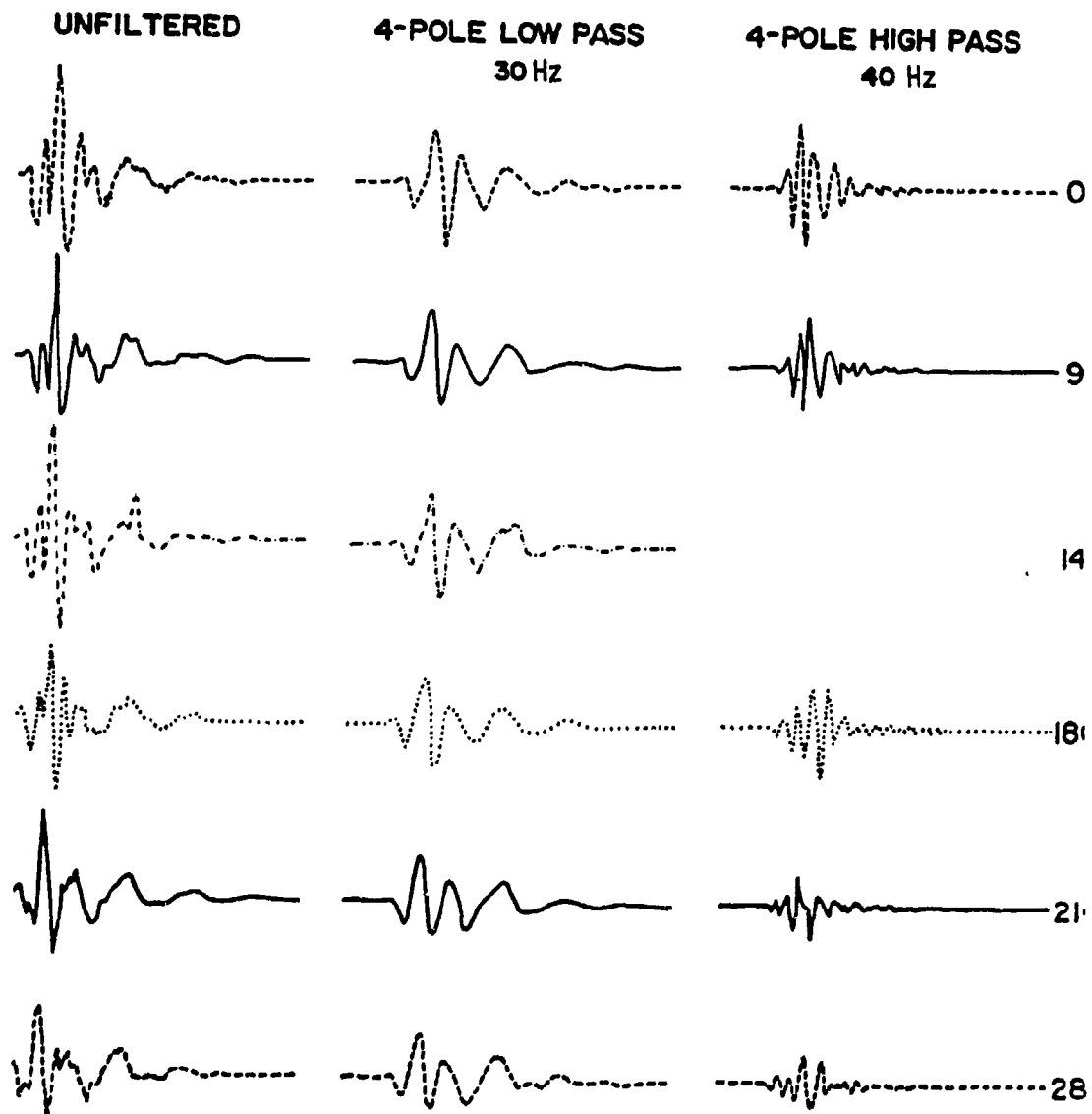


Figure 2. Filtered vertical acceleration records from ART 2.

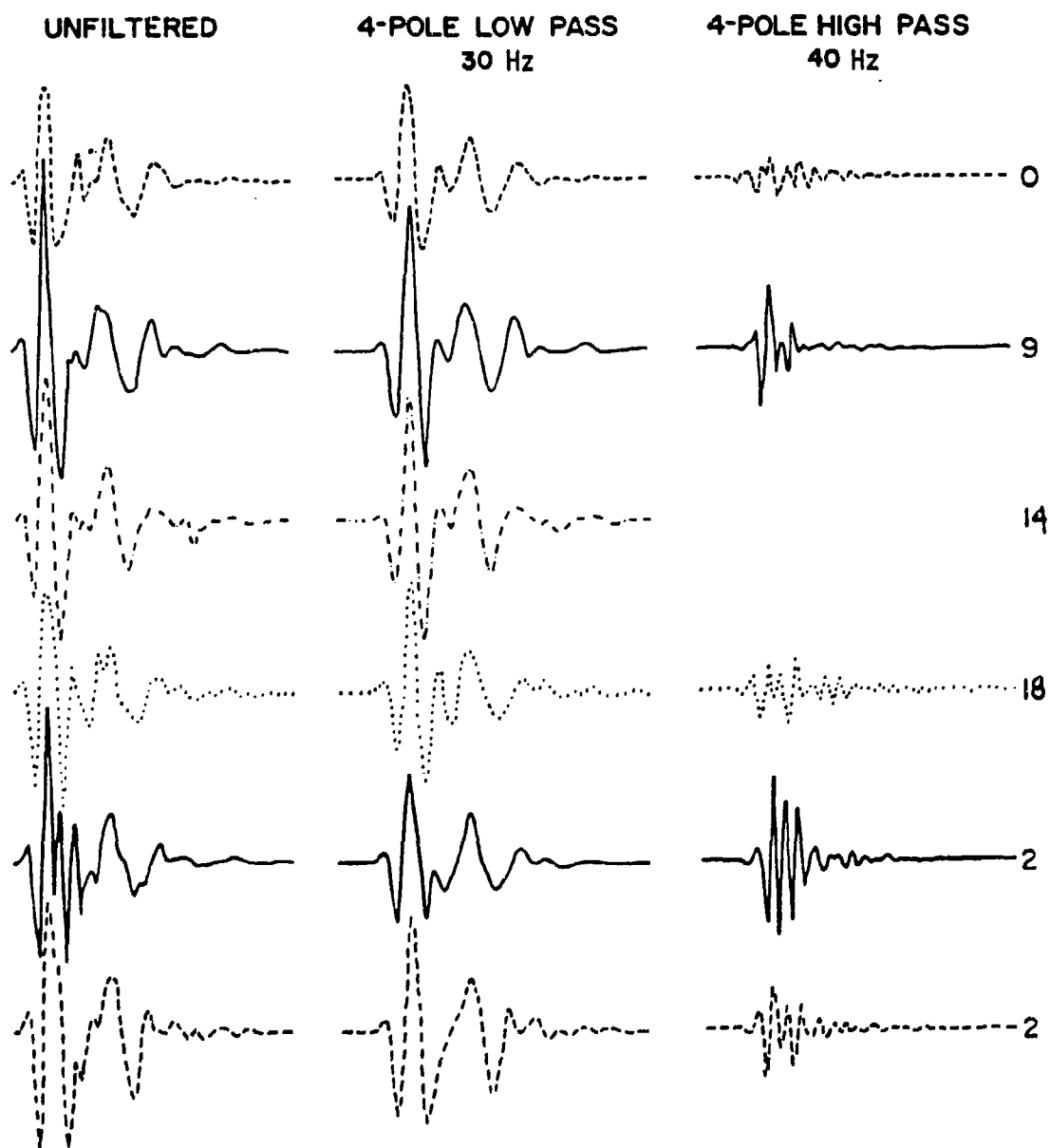


Figure 3. Filtered radial acceleration records from ART 2.

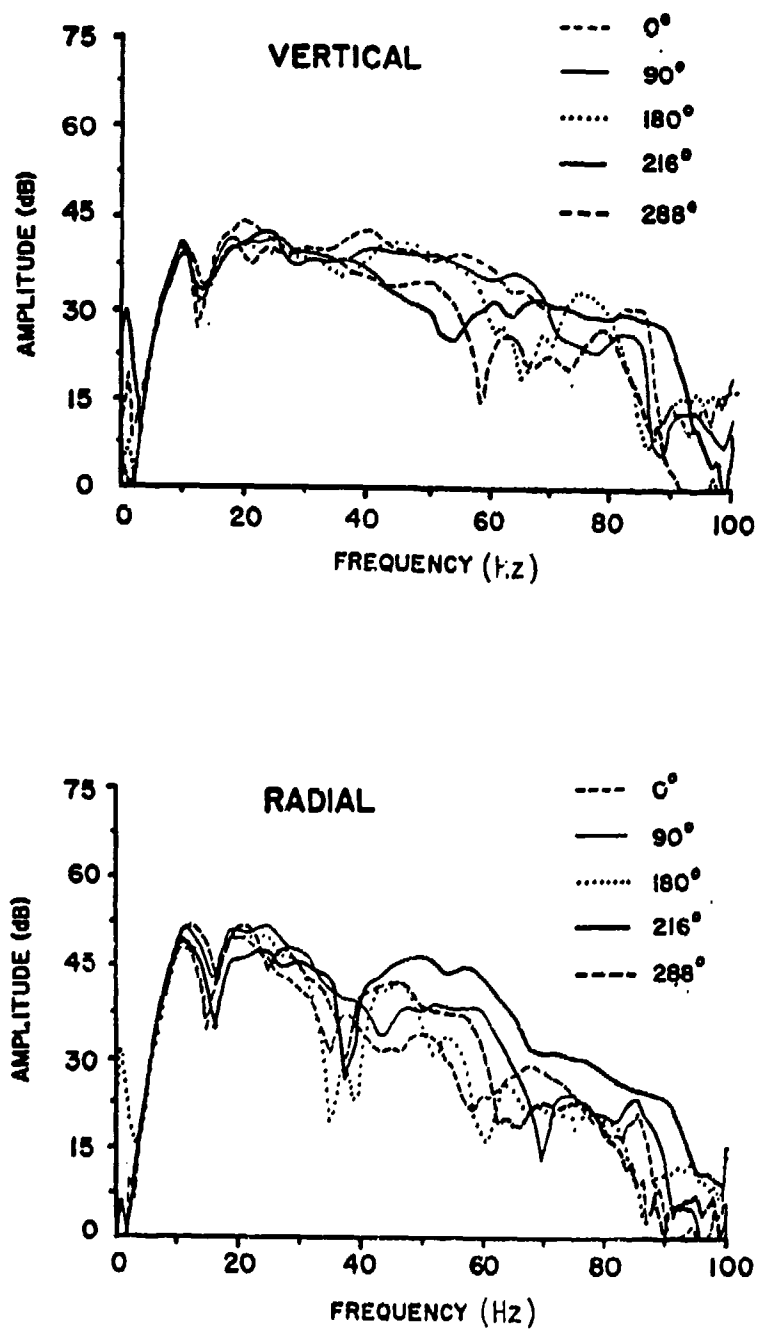


Figure 4. Vertical and radial Fourier acceleration spectra for ART 2.

## EXPERIMENTAL DESIGN

Three possible sources for the observed azimuthal variations in waveforms have been identified: (1) nonuniformity in instrumentation response, (2) asymmetry in the explosive source, and (3) geologic inhomogeneity. In order to experimentally investigate the first possibility--instrumental irregularity--the ART 19 test (Table 1), also called the "huddle" test, was performed. In this test, all seven 3-component accelerometers were placed in a closely spaced group at the 20-m range (Fig. 5) from a 5-lb charge detonated at a depth of 1 m. Individual vertical and radial spectra from this test are compared in Fig. 6. The resulting spectral scatter, as observed in these figures, is at most 3 to 4 dB, over the band from 5 to 70 Hz--much less than that observed for the azimuthal data. In fact, the higher frequency scatter (40 to 70-Hz region) shown in these figures may not reflect true instrumental irregularity, since, as seen by examination of Figs. 5 and 6, the accelerometers which are physically closest together in the field do possess the greatest degree of similarity in spectral shape.

An additional set of experiments, the ART II series (Table 1), was designed to determine whether azimuthal irregularities in ground motion result primarily from propagation path variations and scattering by geologic inhomogeneity or explosive source asymmetry. The test-bed layout for the ART II tests is shown in Fig. 7. Ground motions were recorded by triaxial servo accelerometers and 3-channel digital event recorders at six equally spaced azimuths at a range of 20 m. The ART II series of tests consisted of five separate 5-lb detonations--all fired at the same test-bed with the accelerometers remaining in the same position from shot to shot. The initial detonation was fired at a depth of 1 m in situ. The resulting crater was then excavated and a new 5-lb charge emplaced in the resulting pit with uniform sand rained around the charge. This process was repeated four times. Thus, the ART II series of tests consisted of five shots, one in situ and four pit shots--all using the same test-bed and an identical recording array.

The goal of the ART II tests was to determine whether source asymmetry or geologic factors were the dominant cause of the observed scatter. By



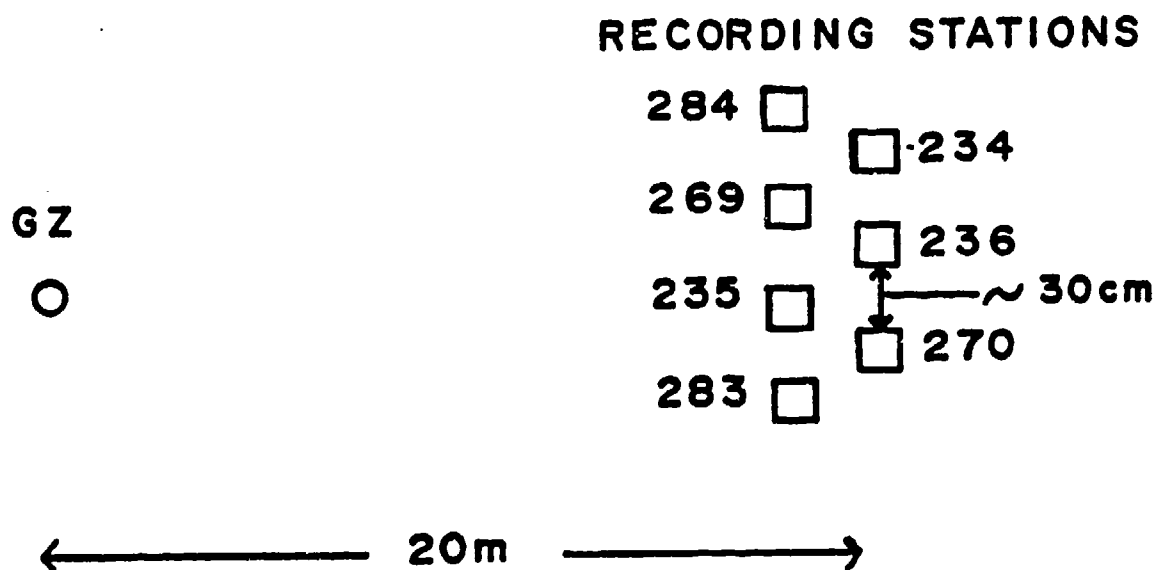


Figure 5. Experimental layout for Huddle Test.

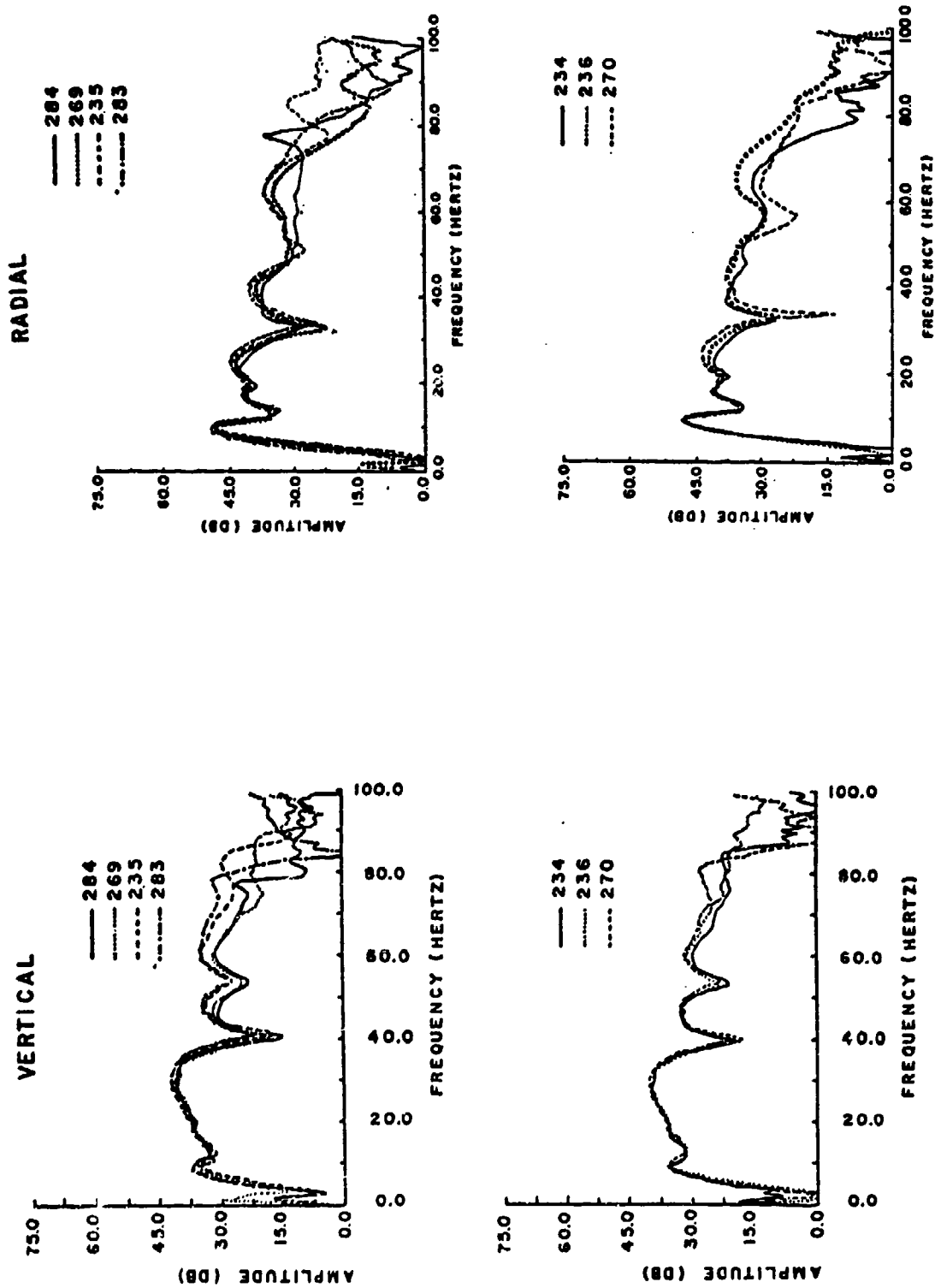


Figure 6. Vertical and radial Fourier acceleration spectra from Huddle Test.

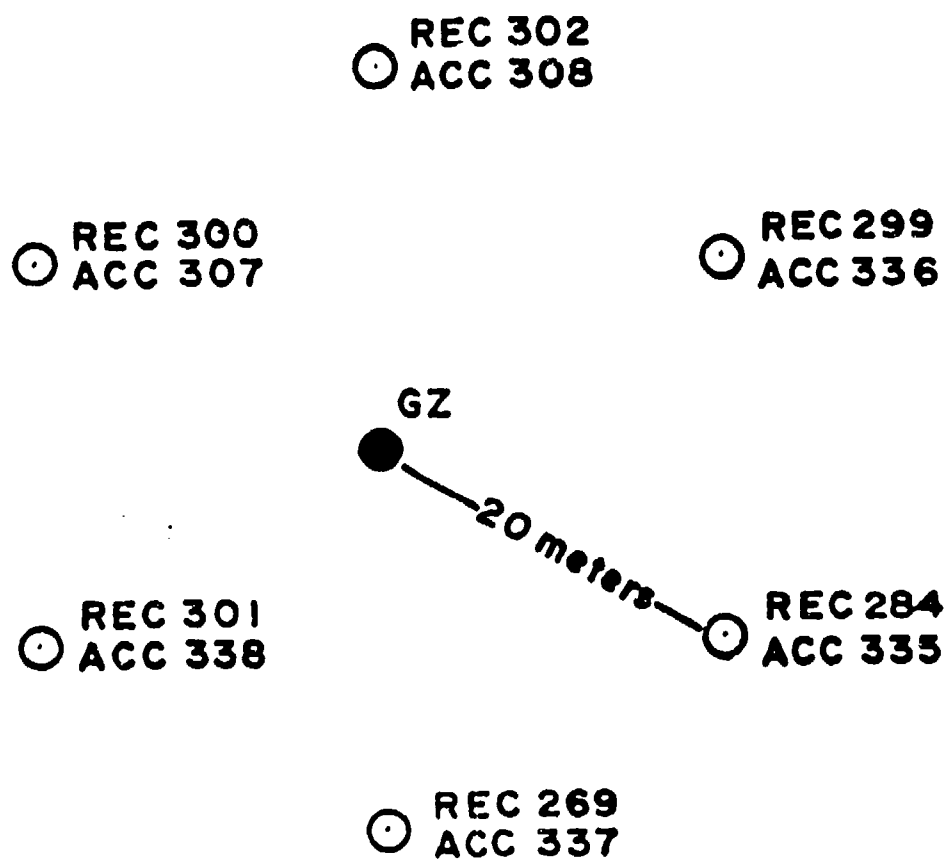


Figure 7. Test-bed layout for the ART II tests.

repeating the experiment five times at the same location, five sets of tri-axial accelerograms and spectra were obtained for each azimuth. If the observed data scatter were produced by geologic inhomogeneity, then one would expect very similar acceleration waveforms, as well as amplitude spectra, to be observed from shot to shot at the same recording station. The detonation of a 5-lb charge is, of course, not strictly a repeatable phenomenon, since the initial in situ detonation destroys a portion of the test-bed by formation of the crater. Excavation of the severely disturbed material comprising the crater and subsequent emplacement of the charge within the pit was intended to make the experiment as repeatable as possible. The transition from the in situ test to the pit sequence was the most severe. The in situ shot produced a crater roughly 2.2 m in diameter. The crater was excavated producing a pit about 3 m in diameter and 1.3 m deep. The dimensions of both crater and pit increased slightly with each shot. The final pit was about 3.5 m in diameter and the final crater about the same diameter.

While the ART 2 and the ART Phase II (the pit shots) experiments investigated azimuthal ground motion variations at the 20-m range, the ART III-1 experiment (Tab. 1) was designed to investigate the influence of range upon the observed azimuthal variations. If scattering by geologic inhomogeneity is the dominant factor producing the azimuthal variation, then one might expect the degree of variation to increase with range of the receiver array. The ART III-1 test consisted of a 5-lb cylindrical charge detonated in situ at a depth of 1 m. The ground motions were recorded at 12 locations using triaxial servo accelerometers and 3-channel digital event recorders. Six recording stations were placed at equal azimuths at the 10-m range, and the remaining six were placed at equal azimuths at the 30-m range.

# STOCHASTIC/DETERMINISTIC CLASSIFICATION TOOLS AND DATA ANALYSIS

One approach to quantify the observed variation in the data sets is to compute the coherency between station pairs in a manner analogous to that employed in Ref. 1. The coherency is defined by

$$\gamma_{xy} = \frac{|\hat{\phi}_{xy}(\omega)|}{\left(\hat{\phi}_{xx}(\omega) \cdot \hat{\phi}_{yy}(\omega)\right)^{\frac{1}{2}}}$$

where  $\hat{\phi}_{xy}(\omega)$  is the cross power spectrum and  $\hat{\phi}_{xx}(\omega) \cdot \hat{\phi}_{yy}(\omega)$  the power spectra of the two time series.

Smoothing must be applied to the spectra prior to estimation of the coherency in order to minimize variances at each frequency. For the coherency estimates computed here, a 4-point lag window was applied to the spectra prior to estimation of the coherency factors.

Coherencies were computed between the 0° data and each of the other recording stations. The time windows used were 128 samples, or 0.64 s in length. This length window encompasses all of the wave train. At this relatively short range, it is effectively impossible to separate the various components of the waveform.

The computed coherencies for the station pairs are shown in Fig. 8. The coherence factors for the vertical and radial components are higher than might be intuitively expected after examination of the spectral plots in Fig. 4. However as noted in Ref. 3, the coherency will be unity when the signals at two stations are related by any linear transfer function, so the coherence function is not a direct estimator of the variation of amplitude across an array.

Based upon the results of the coherency analysis, an alternate approach for analysis of the data was taken. The set of amplitude spectra of the azimuthal observations was treated as a statistical ensemble. Figure 9 gives

## COHERENCE WITH 0° DATA

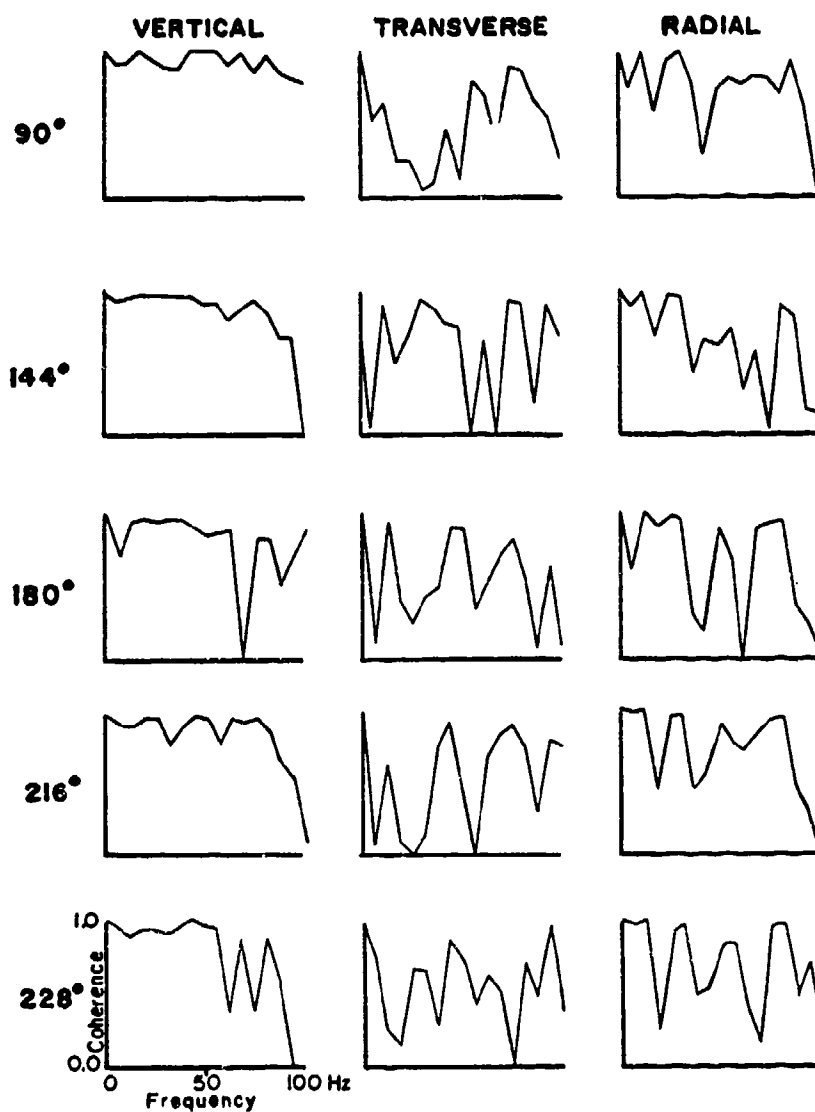


Figure 8. Computed coherencies for ART 2.

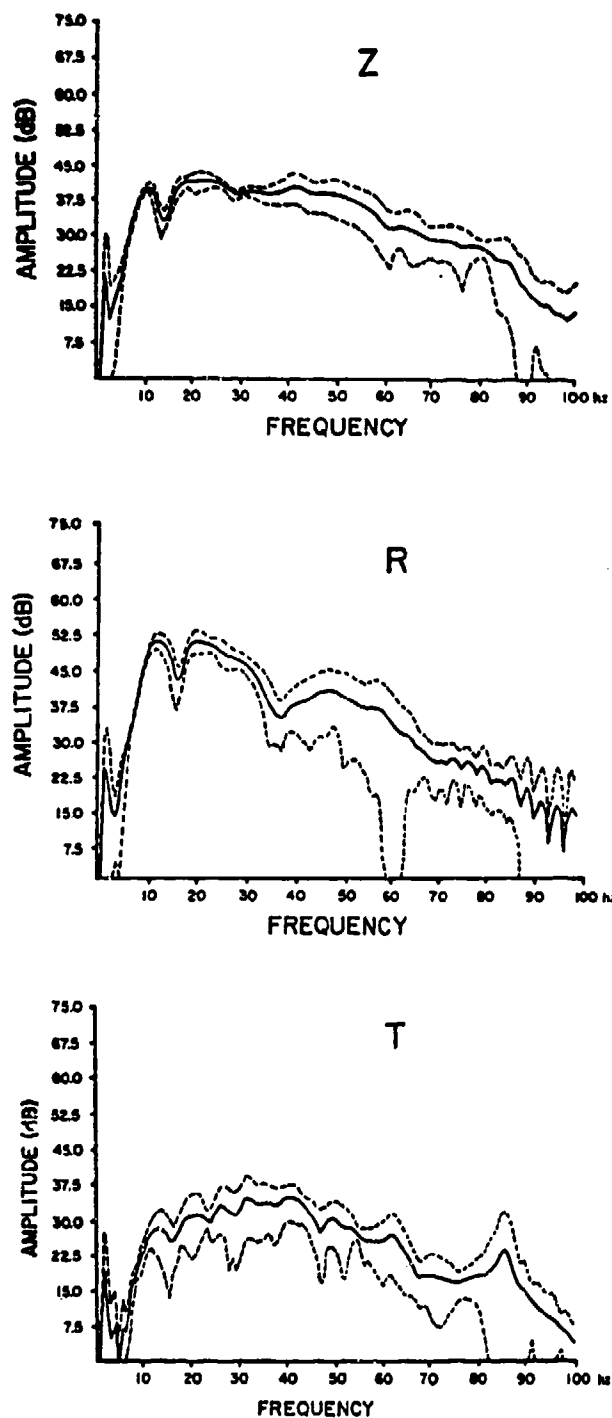


Figure 9. Mean and variance of ART 2 spectral ensembles.

an example of this technique applied to the ART 2 data. The mean and variance of the spectral ensemble were calculated as shown, assuming a lognormal distribution. These figures illustrate  $\bar{\mu}$ , the mean, and  $\bar{\mu} \pm \sigma$ , the mean  $\pm 1$  standard deviation for the vertical, radial, and transverse data from ART 2. The vertical and radial data show small standard deviations between 5 and 30 Hz. Beyond 35 Hz, the width of the  $\bar{\mu} \pm \sigma$  deviation band increases until, at 40 Hz, the expected scatter in the Fourier modulus is 8 dB or greater. The transverse motions, on the other hand, show at least 8-dB scatter throughout the entire frequency band; although the overall mean amplitude is reduced about 10 dB from the radial and vertical amplitude levels. The lack of coherence below 5 Hz on all components has several possible sources. This effect was first thought to be due to signal-induced tilts in the accelerometers. Integration of the acceleration traces and subsequent attempts to correct the resulting velocity and displacement records did not significantly change the estimates. Aliasing and/or noise may be the cause of this low-frequency incoherence. The amplitude level in this region is very low relative to the higher frequencies. Even a small amount of aliased energy would significantly affect the apparent coherence in this region which is well below the corner frequency of the 5-lb source. At higher frequencies the aliased energy level is insignificant relative to the amplitude of the direct source energy.

Another measure of the data scatter in the frequency domain is the coefficient of variation (CV) (Ref. 6). The CV is the ratio of the standard deviation to the mean,  $CV = \sigma/\bar{\mu}$ . The CVs for the ART 2 spectra are given in Fig. 10. For ART 2, the CV on the radial and vertical components increases with frequency ( $CV < 0.5$  from 5 to 30 Hz); the transverse component CV remains approximately constant at a relatively high level ( $> 0.5$ ) across all frequencies, suggesting that the transverse component is uncorrelated at all frequencies. By way of contrast, Fig. 11 shows the very low values of the CV between 5 and 60 Hz for the radial and vertical components of the Huddle (ART 19) test. The advantage of the CV as an estimator of the data scatter across the array is that all stations in the array may be used in the single estimate, as opposed to only a pair of stations in the coherence estimate.

Amplitude spectra of the vertical acceleration waveforms recorded at the 0° azimuth for all five of the ART II pit shots are compared in Fig. 12.



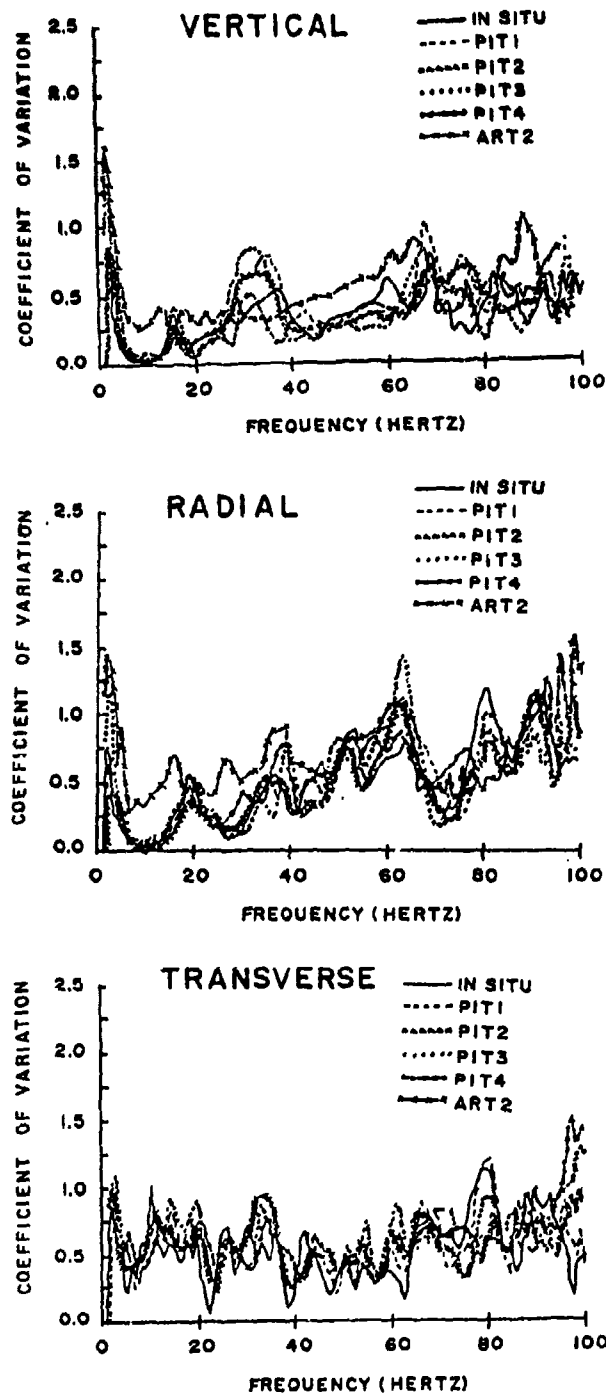


Figure 10. Spectral coefficient of variation curves for the ART II pit shots compared with ART 2.

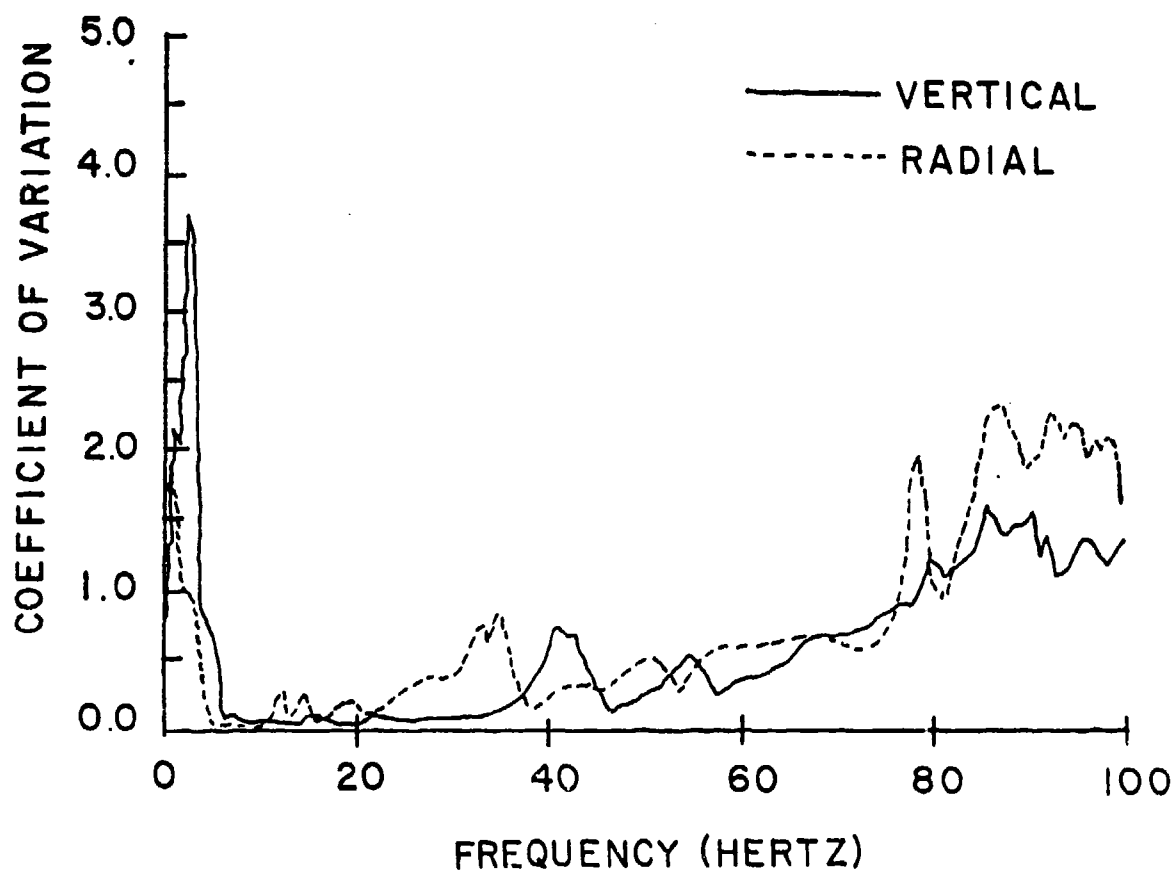


Figure 11. Spectral coefficient of variation curves for the vertical and radial components of the Huddle Test.

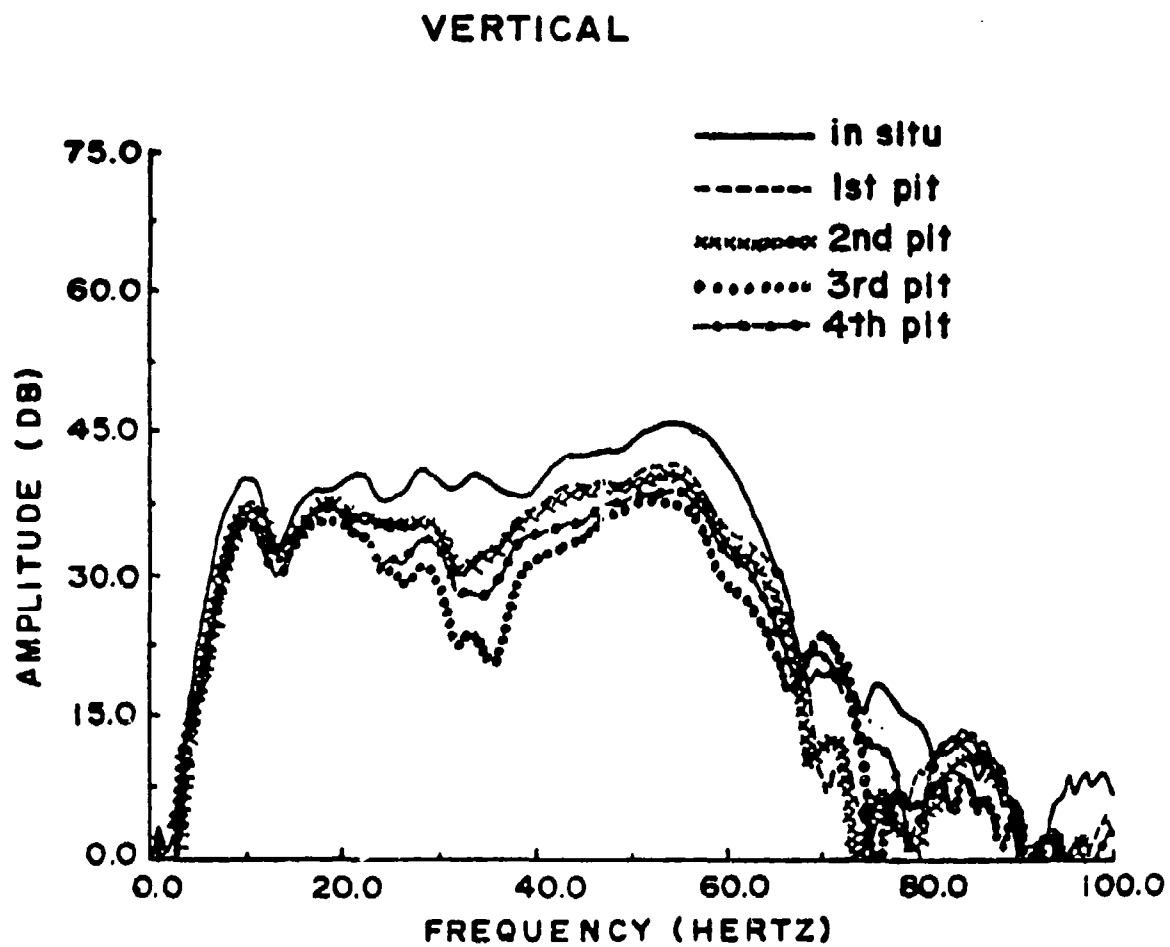


Figure 12. Comparison of vertical acceleration spectra for the five shots of the ART II series.

The sets of spectra recorded at the other azimuths and the other components are similar in character to the 0° vertical set. The four pit shot spectra are quite similar in shape and amplitude, while the in situ shot spectrum exhibits a shape which is similar to that of the pit shot spectra, but higher in amplitude for almost all frequencies. Two of the pit shots are almost identical in the frequency domain; pit shots 3 and 4 also group closely together over most of the frequency band. The greatest change in amplitude from shot to shot occurs in the 30 to 35-Hz region. This area of the spectrum is fairly flat for the in situ shot; however, a spectral hole develops for the pit shots and deepens with each successive pit shot. Even though the shape of the source spectrum may change from shot to shot (which is to be expected since introduction of the backfilled cavity results in more energy lost in cratering, greater attenuation and a larger cavity), the CV should change very little if the source remains cylindrically symmetric for all shots. Figure 10 shows the azimuthal coefficient of variation plotted as a function of frequency for the vertical, radial and transverse components, respectively, for all five shots. The normalized standard deviation curves are very similar for all five shots out to the system anti-alias filter at 70 Hz. The coefficient of variation curves from ART 2, which was conducted near the pit shot site but on a different test-bed, are also plotted in this figure. The change in the coefficient of variation curves between the two sites is much larger than the variation from shot to shot for the pit shot sequence. The relatively small scatter in the coefficient of variation curves for the five events of the pit shot sequence (the in situ shot plus the four pit shots) suggests that source asymmetry plays an unimportant role in the development of the azimuthal variation in ground motion response.

The ART III-2 (Table 1) shot was designed to determine the degree to which azimuthal variation increases with range from the source. In this test, ground motions were recorded by circular arrays at both the 10-m and 30-m ranges. Coefficient of variation plots for the vertical, radial and transverse spectra for both the 10-m and 30-m ranges are given in Fig. 13. These results support the contention that the coefficient of variation increases with range.

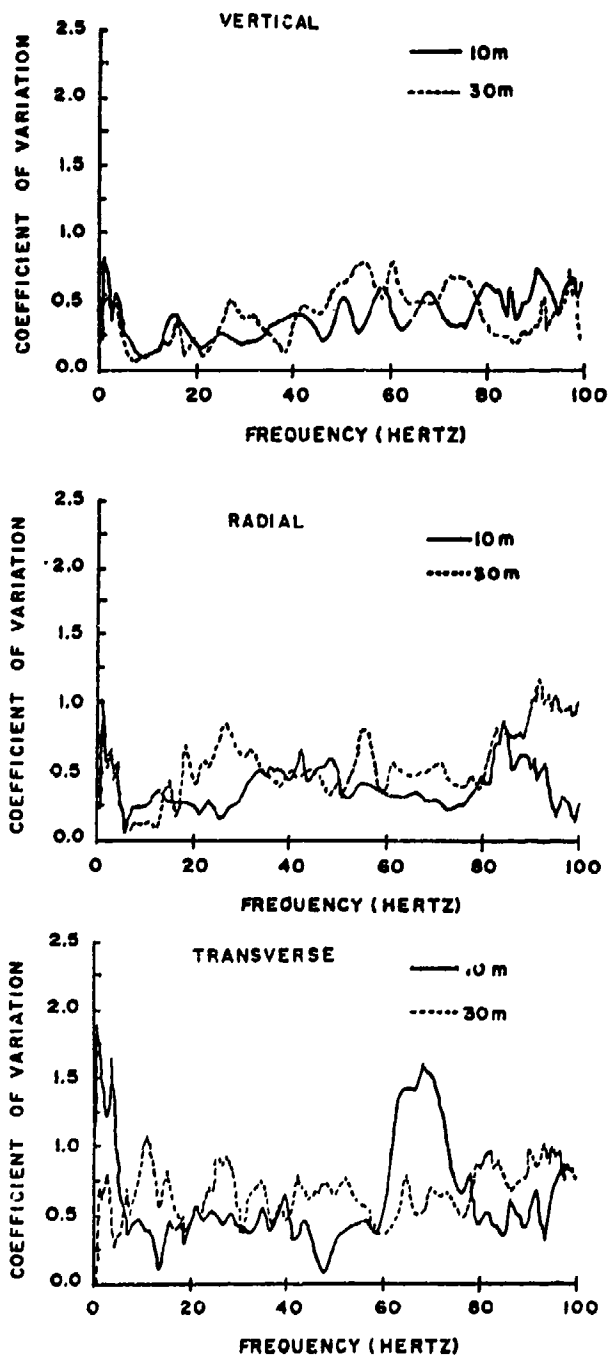


Figure 13. Comparison of 10-m and 30-m coefficient of variation curves for ART III 2.

## NEW SITE CHARACTERIZATION PROCEDURE

One goal of this study is the development of a standardized survey technique which can characterize the degree of geologic inhomogeneity present and its influence upon azimuthal ground motion variations across a site. Such a technique requires a fairly energetic seismic source which is both cylindrically symmetric and repeatable. The Betsy Seisgun\* was chosen for testing as a potentially useful source for these sorts of surveys. The Betsy device is an 8-gauge industrial shotgun converted for use as a seismic source. The Betsy fires an 3-oz slug into the ground surface, providing a fairly energetic seismic source. In order to quantify this source, a series of tests similar to those conducted with the 5-lb charges was performed with the Seisgun.

Seisgun tests were performed within the ART alluvial test site at two different locations about 500 m apart. One of these sites was the same test-bed which was subsequently used for the ART III 10-m and 30-m array tests. This site will be referred to as the ART III site; the other site will be referred to as Site A. All Seisgun tests used vertical 4.5-Hz natural frequency geophones as motion sensors. The geophones were recorded by a 24-channel digital seismic recording system at a sample rate of 0.25 ms, with an anti-alias filter corner at 1000 Hz.

Two separate arrays were employed at Site A. One array was composed of 12 geophones spaced at 30-deg angles at the 20-m range from the Betsy. The other array consisted of a "Huddle" test in which all 12 geophones were placed in a closely spaced group in order to determine the uniformity of instrument response.

One objective of the Seisgun tests at Site A was to determine the repeatability of the signal from shot to shot. Figure 14 illustrates the mean and variance of the amplitude spectrum as recorded at a single station for four successive shots of the gun at Site A. The signal is quite repeatable from

---

\*Betsy Seisgun is a trademark of Betsy Seisgun, Inc, Tulsa, OK.

\*\*To convert from oz to kg, multiply by 2.834 952 E-02.

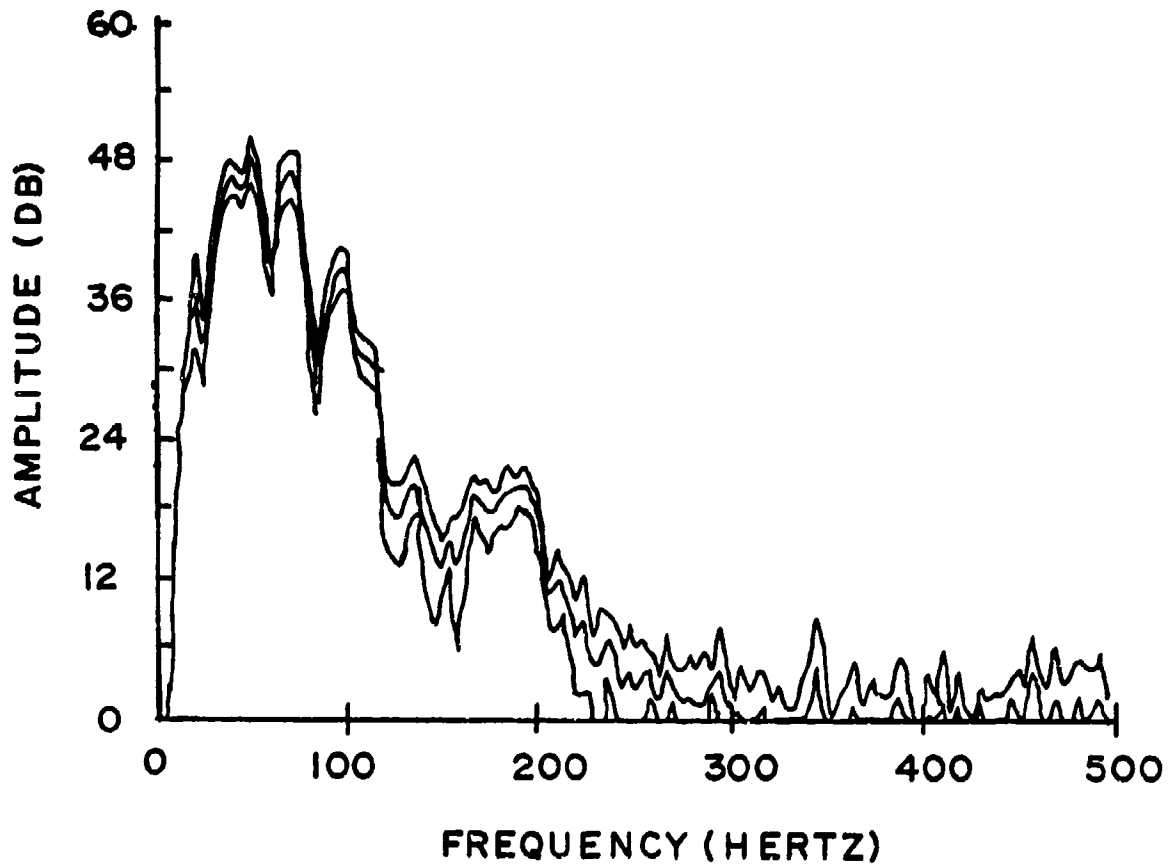


Figure 14. Mean and variance of spectra for four shots of the Seisgun at the same site.

shot to shot. These shots were the sixth, seventh, eighth, and ninth firings into the same hole (i.e., the gun was fired five times prior to the first recording in order to establish proper gain levels on the recording system). The signal may not be as repeatable for the first few shots into the same spot because of changing source characteristics as the hole dug by the slug becomes deeper.

Figure 15 compares the coefficient of variation of the amplitude spectrum for the "Huddle" test with the coefficient of variation computed for the full 12-channel circular array test at Site A. The full array coefficient of variation is perhaps 0.3 to 0.4 greater above 35 Hz than that observed in the "Huddle" test, again implying that the observed azimuthal variations in amplitude levels for the full circle array test at Site A are not due to instrumental irregularity.

A number of tests were conducted with the Seisgun at the ART III site. Recordings were made at the 10-m, 20-m, and 30-m ranges. Twelve vertical geophones were positioned at 30-deg increments at each range. Recordings were performed for several shots of the gun with a total of 24 geophones at the 10-m and 20-m ranges. The 10-m phones were then shifted to the 30-m range and several more shots were recorded. Objectives of these gun tests were: (1) to determine repeatability of array coefficient of variation data for several shots of the Seisgun, both into the same hole and when the position of the Seisgun is shifted slightly from the original shotpoint, and (2) to determine how the coefficient of variation changes with increasing range (unfortunately, we were not able to record unclipped waveforms at the 10-m range).

Figure 16 contains a comparison of the 20-m coefficient of variation for three Seisgun shots at the ART III site and one shot at Site A. The coefficient of variation curves for the three shots at the ART III site are quite similar, particularly at the lower frequencies. The Site A curve diverges fairly widely from the ART III curve above 30 to 40 Hz (at 60 Hz the Site A curve approaches a CV value of 1.0 while the ART III CV is near 0.5), indicating the difference in degree of geologic scattering between the two sites. Two of the ART III curves in Fig. 16 are from the 7th and 22nd shots fired



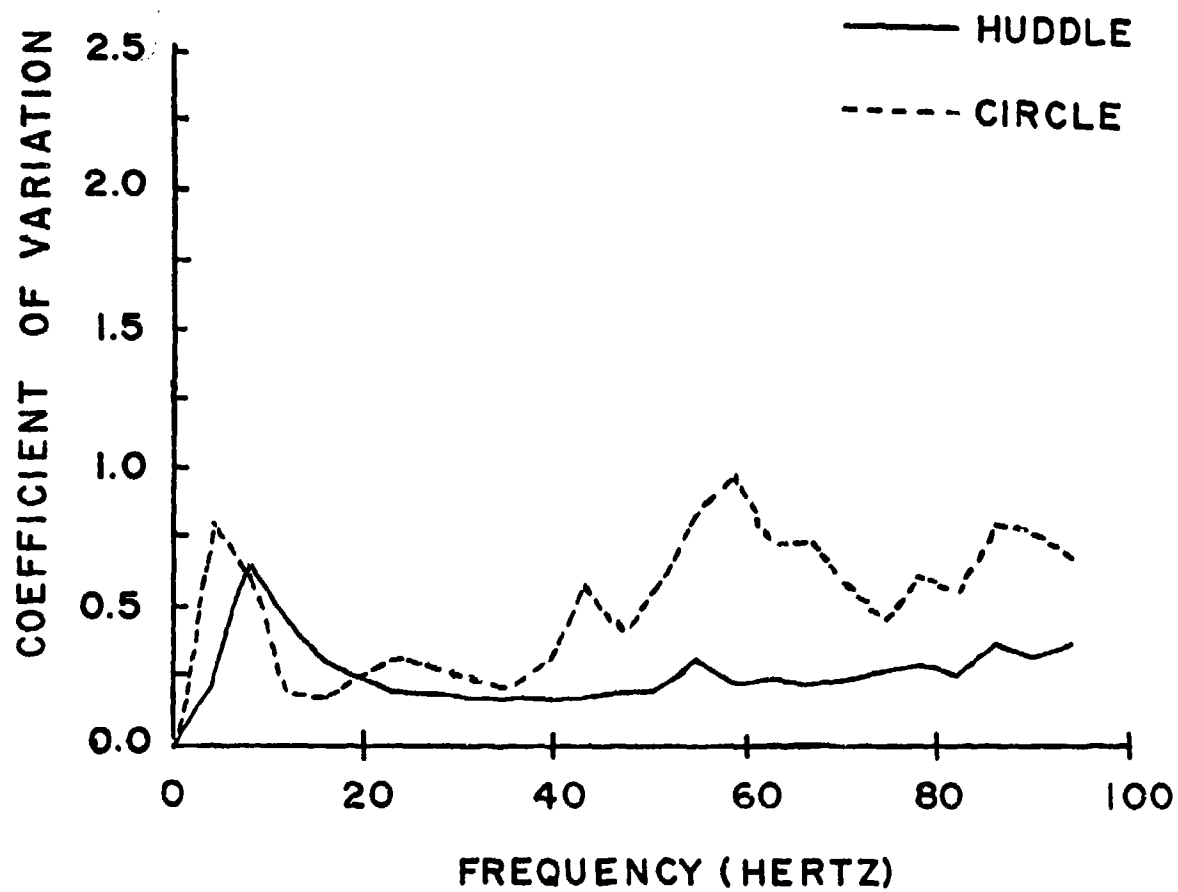


Figure 15. Comparison of Seisgun Huddle Test coefficient of variation with full circle array coefficient of variation.

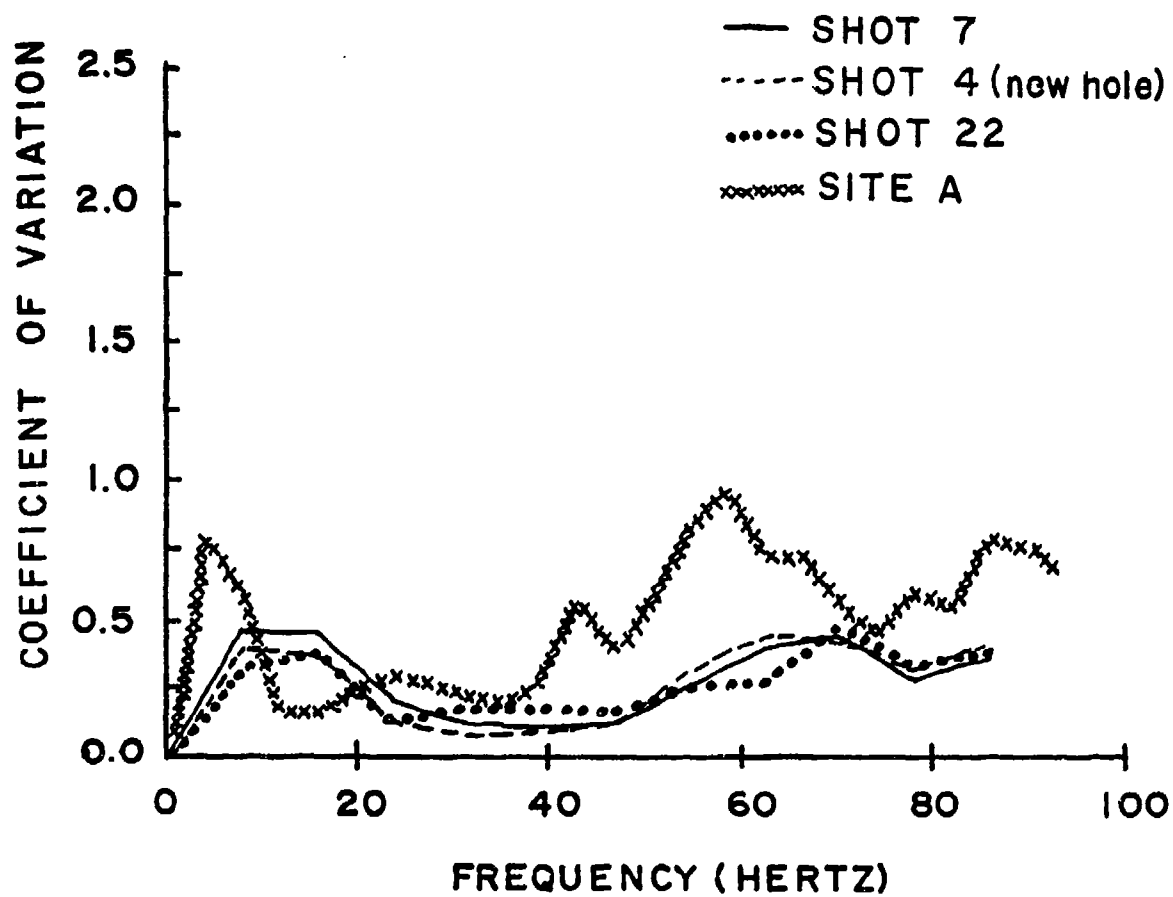


Figure 16. Comparison of the coefficient of variation curves for three Seisgun shots at the ART III-2 site and one shot at Site A.

into the same hole; the remaining curve was obtained from the 4th shot fired into a point on the surface which was displaced approximately 0.5 m from the other shotpoint. The excellent agreement between the curves obtained from the two different shotpoints shows that the observed azimuthal variations are indeed a result of geologic scattering and not source irregularity or asymmetry. In Fig. 17, a comparison is made between the coefficient of variation curves obtained from the 20-m and 30-m circle arrays at the ART III-2 site. As in the ART III 5-1b CV comparison (Fig. 13), the CV values for the larger range circle array are higher over most of the frequency band than the close-in array values. This increase of azimuthal variability with increasing range from the source is what would be expected for scattering due to geologic inhomogeneity.

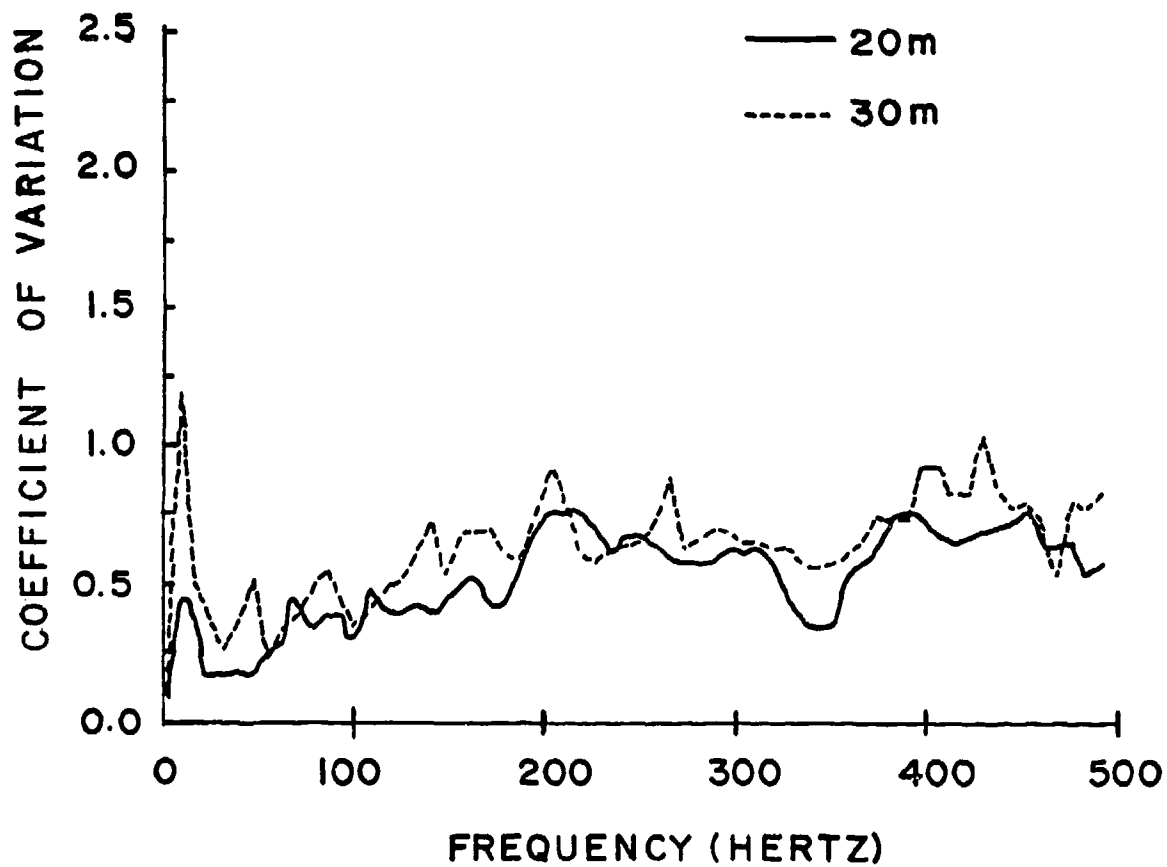


Figure 17. Comparison of 20-m and 30-m coefficient of variation curves for the Seisgun.

## RELATION OF OBSERVED AZIMUTHAL VARIABILITY TO TEST SITE GEOLOGY

The tests discussed in this report were conducted at the same test site in the Rio Grande Valley south of Albuquerque, New Mexico. The subsurface geology consists of dry alluvium down to the water table at a depth of approximately 75 m. The site lies in a small shallow basin which in earlier times contained a playa. In general, the site is underlain by unconsolidated eolian sands, alluvium and lacustrine deposits 15 to 30 m thick. Beneath this material are the tertiary Santa Fe and Galisteo formations, 180 to 300 m thick (Ref. 7). A typical near-surface P wave velocity section is shown in Fig. 18 (Ref. 8).

Near-surface deposits are fairly variable with intermittent caliche beds present. Trenching at other test sites in the area has revealed discontinuous subsurface caliche beds typically on the order of 0.5 to 1.0 m in thickness (Ref. 8). In an effort to quantify the nature of the subsurface variability at the ART 2 test site, 18 boreholes were drilled within the confines of the test-bed (Fig. 19). Each borehole was drilled to a depth of 6.1 m. Standard penetration tests in each hole determine the number of hammer blows required to drive a sampling tube a unit distance. This blow count is related to the in situ density and compressive strength of the subsurface material (Ref. 9). Figure 20 displays the blow counts per meter for each borehole down to the 6-m depth. Figure 19 contains isopach maps showing the lateral distribution of the areas of similar blow counts as a function of depth.

A thorough understanding of the physical processes responsible for the observed azimuthal variability in the ART 2 test requires that a quantitative relationship be established between the subsurface material property information and the observed ground motion characteristics. Aki and Richards (Ref. 10) present such a relationship. Following Chernov (Ref. 11), they characterize the statistical nature of geologic media by the autocorrelation of the velocity fluctuation.

For  $u = -\delta C/C_0$ , where  $C_0$  = velocity, the normalized autocorrelation function is defined by

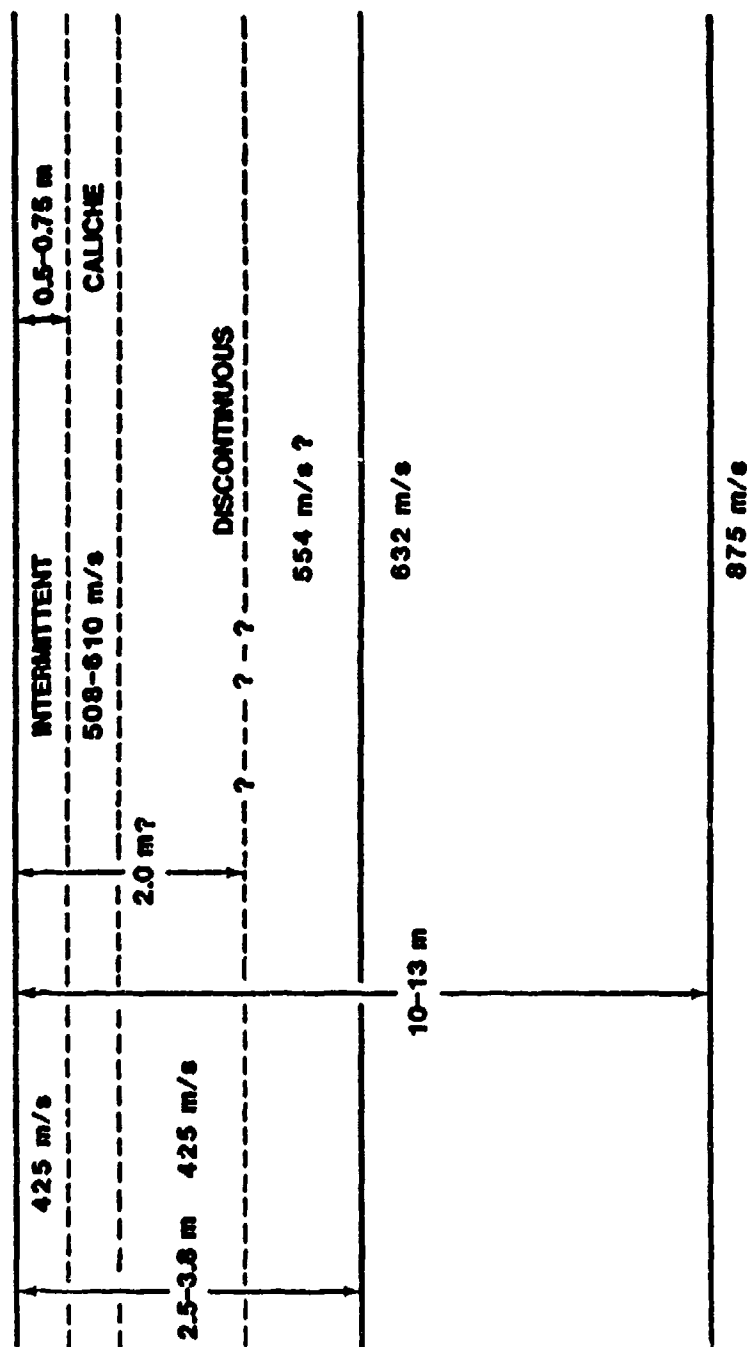


Figure 18. Generalized geologic cross section of McCormick Ranch.

## PENETRATION TEST — ARTS

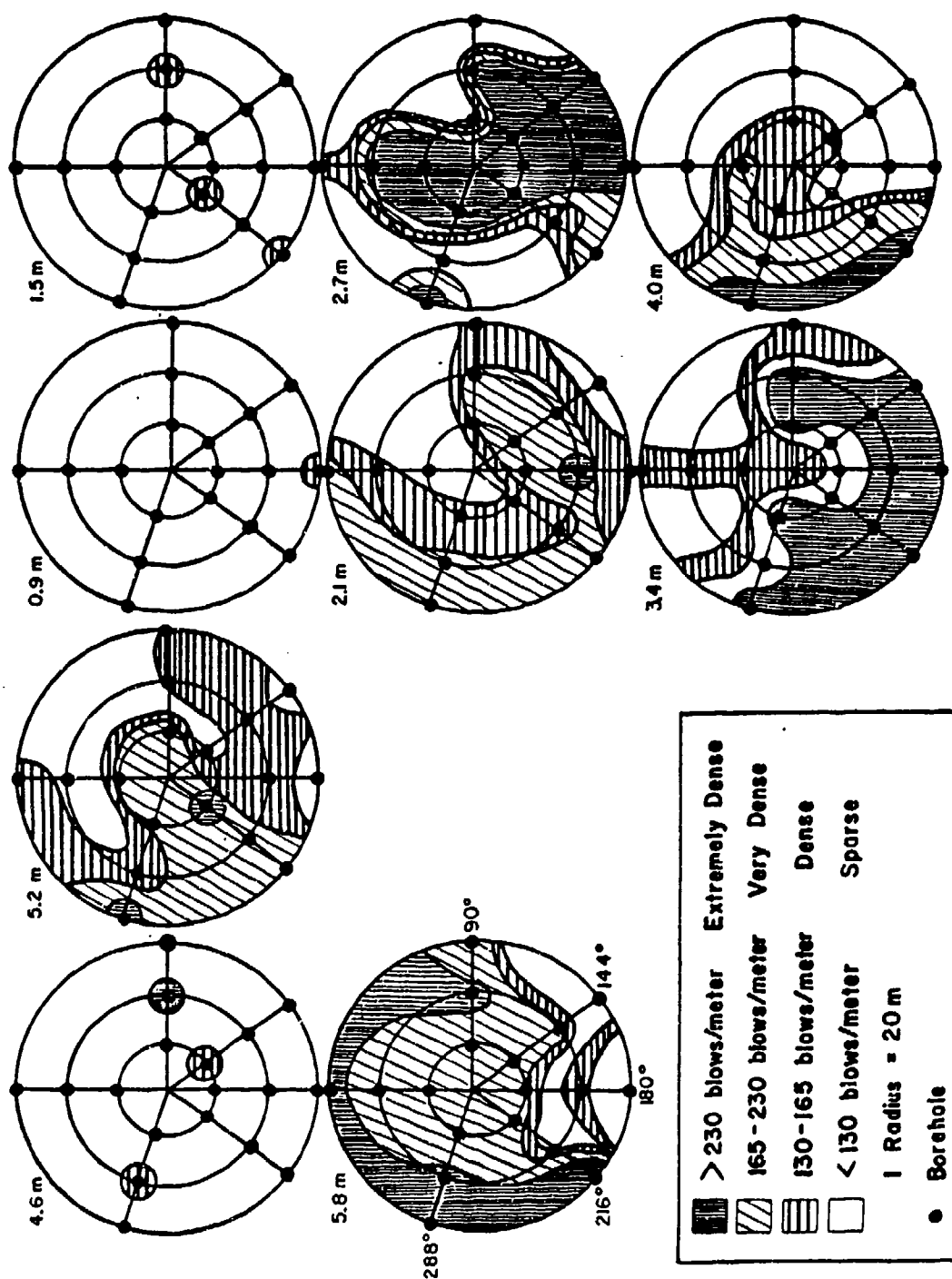


Figure 19. Layout of boreholes within the ART 2 test-bed and isopach map of blow counts.

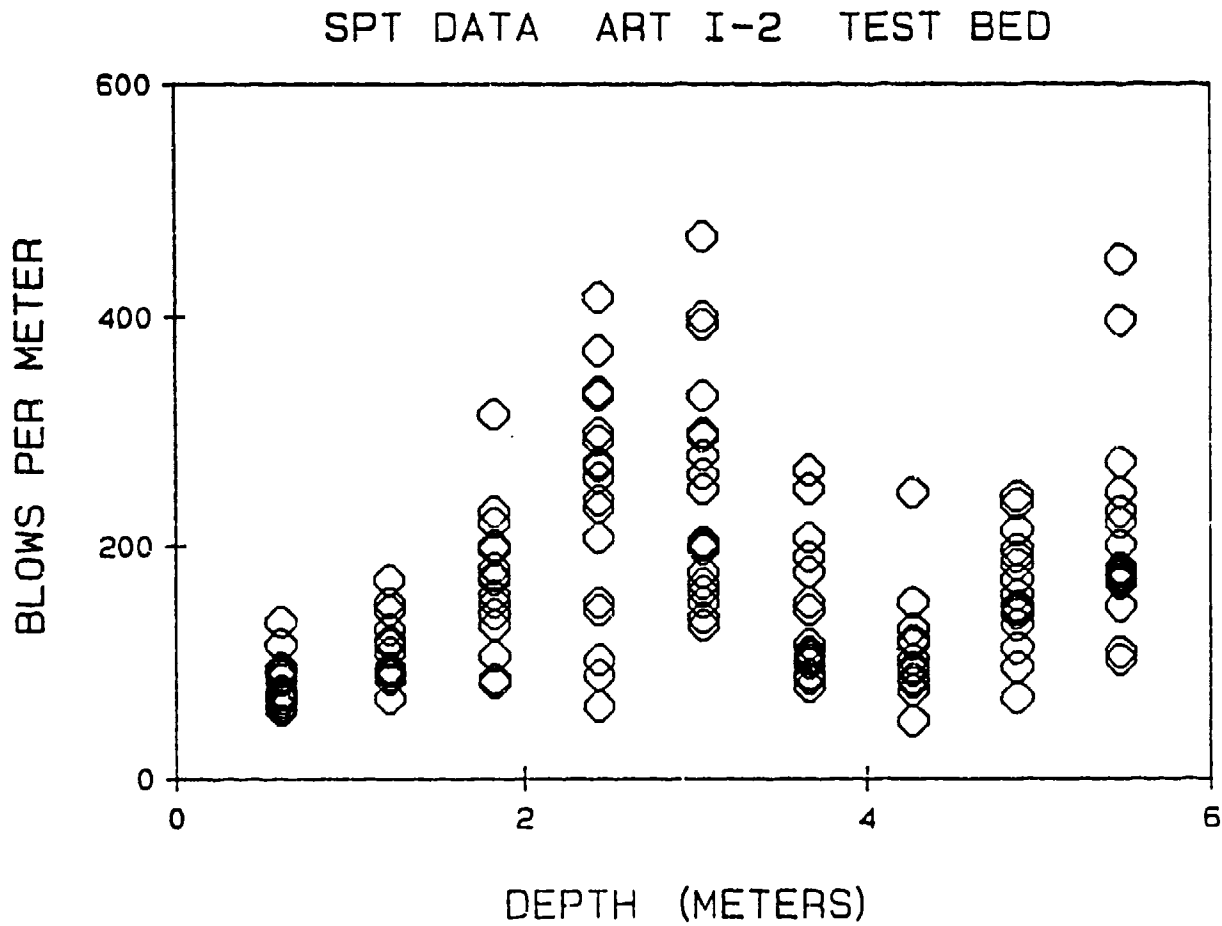


Figure 20. Plots of blow counts vs depth (data points from all 18 boreholes are included).



$$N(r) = \langle \mu(r') \cdot \mu(r'+r) \rangle / \langle \mu^2 \rangle$$

where  $r$  denotes position.

Two statistical distributions are considered: (1) the case where  $N(r) = e^{-|r|/a}$  (exponential distribution), and (2) the Gaussian distribution given by  $N(r) = e^{-r^2/a}$ . The quantity  $a$  is the measure of scale length of the medium inhomogeneity called the correlation distance.

Once a medium is described statistically in terms of  $N(r)$ , then the Born scattering approximation may be used to determine the strength of the scattering as a function of frequency for the medium. Following Ref. 10, the ratio of scattered energy to total energy is given as follows:

$$\delta I/I = 8\langle \mu^2 \rangle \cdot k^4 \cdot a^3 \cdot L \text{ for } ka < 1$$

and

$$\delta I/I = 2\langle \mu^2 \rangle \cdot k^2 \cdot a \cdot L \text{ for } ka > 1.$$

where  $\delta I/I$  is the ratio of scattered energy to the total energy carried by the wave,  $\langle \mu^2 \rangle$  is the average of the square of the velocity perturbation,  $K$  is the wave number,  $a$  is the scale length or correlation distance of the medium, and  $L$  is the length of the travel path.

Making the assumption that there is a linear correlation between the blow count value at a particular point and the P wave velocity at the same point, we shall attempt to relate the observed azimuthal variability in the ART 2 data with the blow count data using the scattering theory discussed above. The mean was computed for the set of blow count data for all of the holes. This yields a mean value of approximately 50 blows/0.30 m. This value was treated as  $C_0$  in the scattering equations. Therefore, the autocorrelation function of the following ratio was then computed:  $(BC_1 - \overline{BC})/\overline{BC}$ , where  $BC_1$  is the individual blow count value, and  $\overline{BC}$  is the mean value of all blow counts. The autocorrelation functions were computed separately for each hole.

Values of the autocorrelation functions of the blow count data for all of the holes are plotted in Fig. 21. Also plotted in Fig. 21 are several theoretical autocorrelation functions for different values of the correlation length  $a$ , for both the Gaussian and exponential distributions. Based on examination of these plots, the theoretical distribution function which best fits the data is apparently an exponential function with a scale length between 2.0 and 3.0 m. This scale length applies, of course, only to the vertical distribution of inhomogeneity. The horizontal inhomogeneity scale length could well be different in character. The horizontal spacing of the boreholes ( $\approx 6.7$  m) is much too wide to allow any sort of reasonable estimate of the horizontal scale length (this spacing yields a nyquist wavelength of 13.4 m).

Using the Born equations, the ratio of scattered energy to total energy,  $(\delta I/I)$ , was computed for the ART 2 test-bed using several values of the inhomogeneity scale length as shown in the plots in Fig. 22. The  $ka \ll 1$  case is appropriate for most of the frequency-scale length combinations under consideration here. The  $ka \gg 1$  case is appropriate for scale lengths greater than 2 m in the higher frequency region ( $>20$  Hz). Both curves indicate that, for scale lengths of 2.0 to 3.0 m, significant  $(\delta I/I > 0.10)$  scattering begins near 10 Hz. Significant scattering in the ART 2 test data occurs above 30 to 35 Hz (Fig. 4). There are several possibilities for this apparent poor correlation: (1) the Born approximation is valid only for small values of scattered energy; (2) the autocorrelation function which was derived pertains only to the vertical distribution of inhomogeneity, and thus the scale length which is appropriate for the overall propagation medium could be considerably different from 2.0 to 3.0 m; (3) a finer spatial sampling of the near surface blow count values might well yield a smaller scale length; and (4) the assumed correlation between blow count data and P wave velocity may be incorrect.

To determine the effect of varying the scale length upon the theoretical scattered energy,  $\delta I/I$  as a function of frequency was computed for correlation lengths of 1.0 m, 0.5 m and 0.25 m (Fig. 22). For these scale lengths, the frequency at which scattering becomes significant is in the 25 to 30-Hz region. This result, particularly the 0.5 curve, correlates much better with the

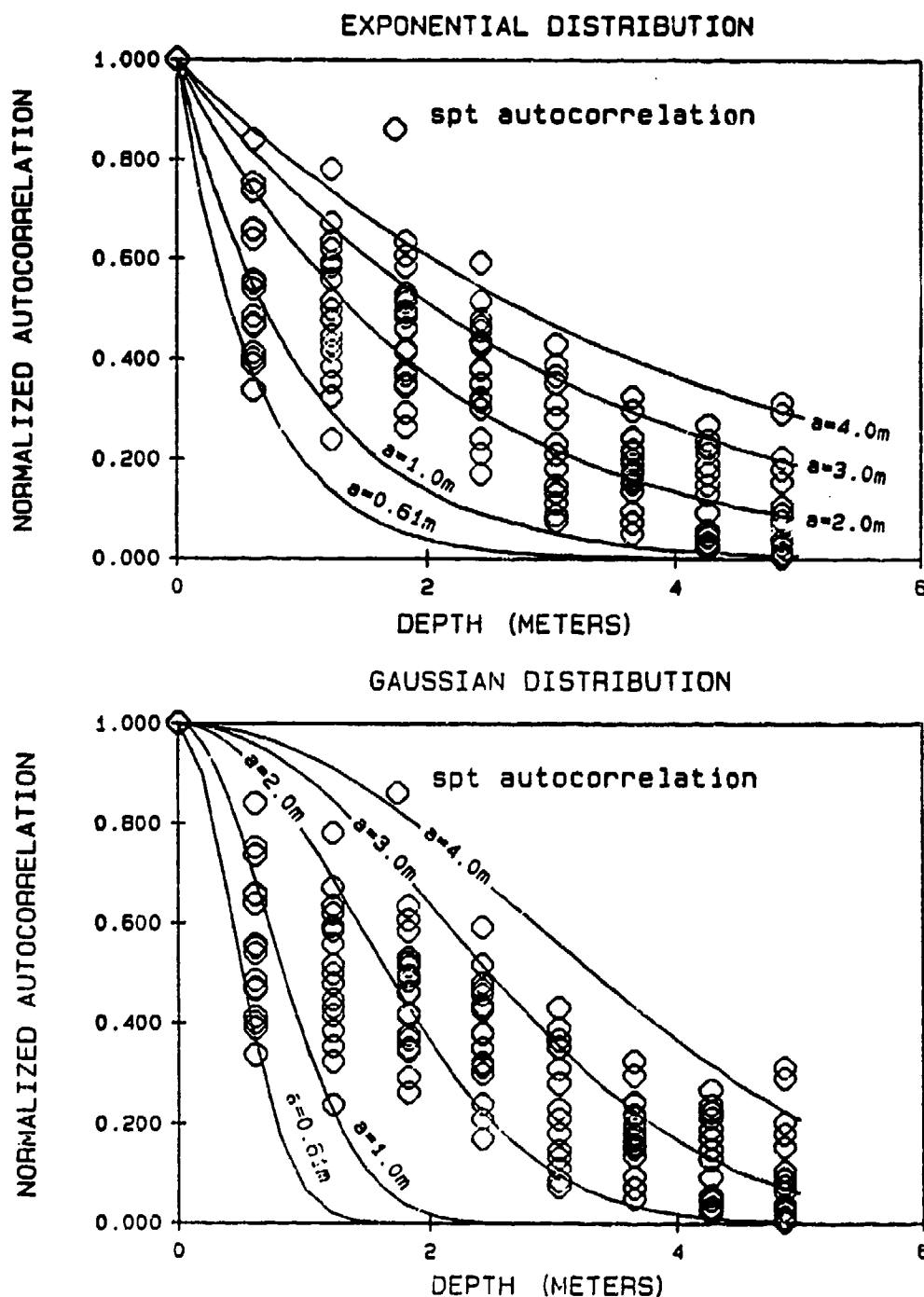


Figure 21. Experimental autocorrelation function compared with Gaussian and exponential autocorrelation functions. (The lines on the plot are the theoretical autocorrelation functions; the experimental autocorrelation functions from all holes are represented by data points.)

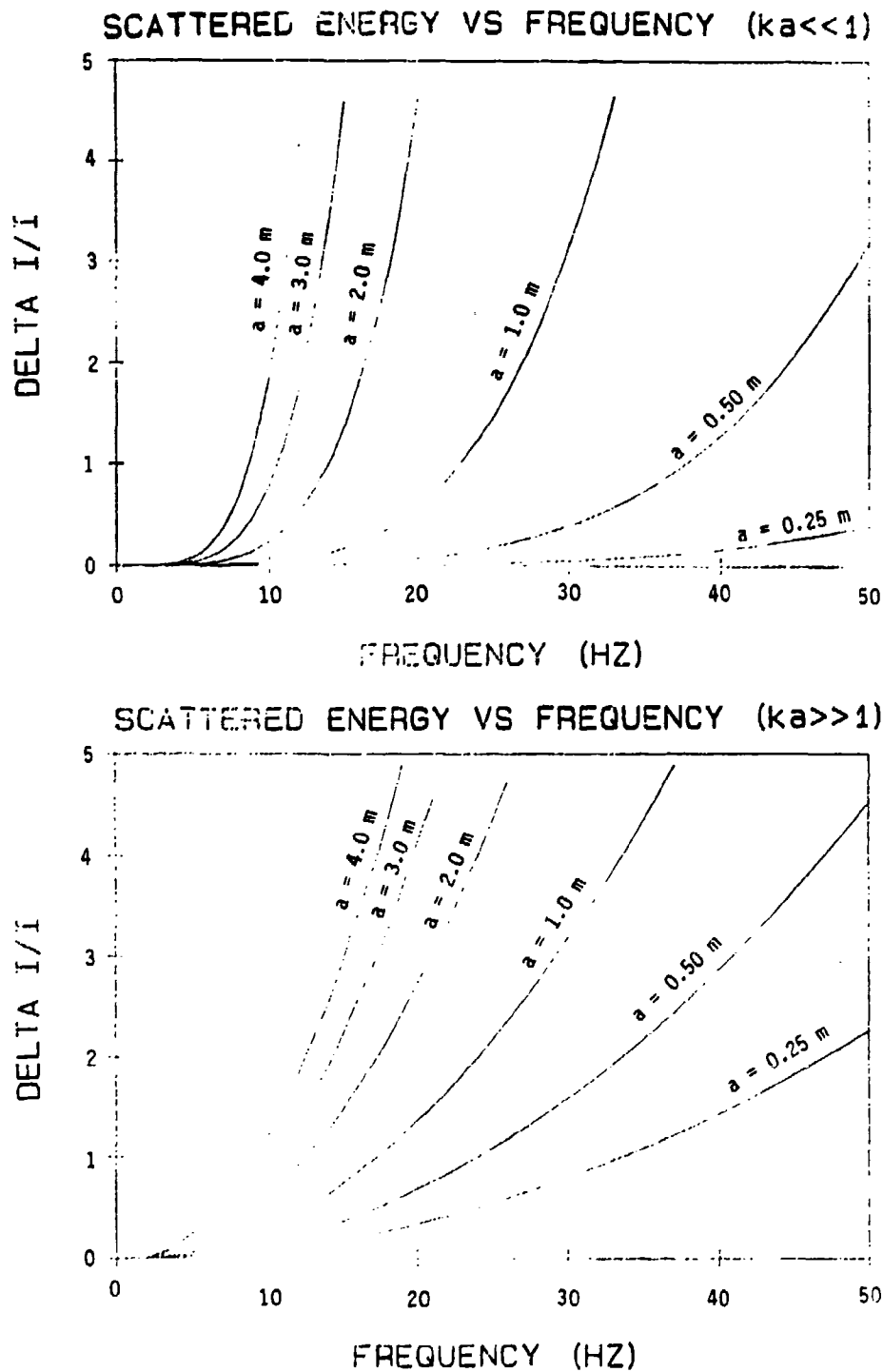


Figure 22. Plot of scattered energy as a function of frequency for different scale lengths.

observed threshold of incoherence in the ART 2 test. A correlation scale length in the neighborhood of 0.5 to 1.0 m is also not unreasonable in light of the results of the "Huddle" test (ART 19) in which all of the instrumentation was placed in a group approximately 1 m wide (Fig. 5). Examination of the spectra from this test in Fig. 6 reveals that the spectra of the endmost instruments separated by a distance of approximately 1 m begin to diverge; whereas, the spectra from instruments spaced more closely correlate very well. Shallow trenching in the general test site area suggests that a typical caliche bed thickness is on the order of 0.5 to 1.0 m, although a typical lateral extent may be slightly greater (Ref. 8).

This simple forward model indicates that the azimuthal variability in the ART 2 data can be explained with a scattering model based upon the Born approximation. The implication is that the particular standard penetration test array did not properly characterize the appropriate scale length due to inadequate horizontal or vertical spatial sampling, since blow count values were obtained by counting the number of blows required to drive the sampling tube a distance of 0.6 m. This sample interval yields a Nyquist wavelength of 1.2 m.

## DISCUSSION AND CONCLUSIONS

The results of the ART experiments combined with the Betsy Seisgun observations have shown, at least for this particular alluvial test site, that the predominant cause of azimuthal variation in ground motion response is inhomogeneity in near-surface geologic material rather than very near-source asymmetry. Considering that this particular site in general is thought to have a fairly uniform near-surface geologic composition, the degree of azimuthal variation observed from these small tests is fairly remarkable. For the short ranges involved here, the 8-gauge shotgun provides a repeatable and symmetric source to be used in the development of a standardized seismic survey technique for characterization of these azimuthal variations. Surveys of this type should be performed at several sites to further constrain the relationship between the spectral coefficient of variation and the variation in the geologic structure. Such surveys will aid greatly in the interpretation and understanding of ground motion data from small-scale field tests. For a small-scale test performed at the ART 2 site, deterministic interpretations of the data cannot be made above the 30 to 35-Hz region. Coefficient of variation surveys could also place limitations upon the interpretation of near source, regional, and teleseismic measurements of earthquakes and explosions made at a single point. These surveys may be useful in explaining the lack of coherence between individual station pairs in small seismic arrays, such as the Pinon Flat array (Ref. 2).

In this study, an initial attempt was made at relating the available subsurface information at the ART 2 site with the observed waveform variation in the test. This attempt was not very successful, probably due to insufficient spatial resolution of the subsurface sampling performed. Forward modeling argues that the scale lengths which are present in the ART 2 test-bed are perhaps on the order of 0.5 to 1.0 m rather than 2.0 to 3.0 m as determined from the autocorrelation of the standard penetration test blow count data. Use of other sampling techniques, such as the seismic cone penetrometer test (in which the force necessary to drive a rod into the ground is measured and a geophone in the rod tip is used to perform a velocity survey), could obtain much finer spatial resolution both horizontally and vertically,

allowing a greatly improved characterization of the random properties of the medium.

## REFERENCES

1. McLaughlin, K.; Johnson, L.; and McEvelly, T.; "Two-Dimensional Array Measurements of Near-Source Ground Accelerations," Bulletin of the Seismological Society of America, Vol. 73, No. 2, pp. 349-376, 1983.
2. Vernon, F.; Fletcher, J.; Haar, L.; Bolswick, T.; Sembera, E.; and Brune, J.; "Spatial Coherence of Body Waves from Local Earthquakes Recorded on a Small Aperture Array," EOS: Transactions of the American Geophysical Union, Vol. 66, No. 46, p. 954 (abstract), 1985.
3. Smith, S.W.; Ehrenberg, J.; and Hernandez, E.; "Analysis of the El Centro Differential Array for the 1979 Imperial Valley Earthquake," Bulletin of the Seismological Society of America, Vol. 72, No. 1, pp. 237-258, 1982.
4. Reinke, R.; and Stump, B.; "Investigation of Azimuthal Asymmetry in Ground Motion Data from Small Scale Explosion Tests in Alluvium," EOS: Transactions of the American Geophysical Union, Vol. 66, No. 46, p. 965 (abstract), 1985.
5. Stump, B.; and Reinke, R.; "Experimental Confirmation of Superposition from Small Scale Explosions," submitted to the Bulletin of the Seismological Society of America, 1986.
6. Bethea, R.; Duran, B.; and Boullian, T.; Statistical Methods for Engineers and Scientists, Marcel Dekker, Inc, New York, 1985.
7. Bedsun, D., "Summary of Geotechnical Testing and Material Models for Subsurface Soil Conditions at McCormick Ranch, Kirtland AFB, New Mexico," Letter Report, NMERI 7.11-TA7-20, 1983.
8. Stump, B.; and Reinke, R.; Spall-Like Waveforms Observed in High Explosive Testing in Alluvium, AFWL-TR-82-15, Air Force Weapons Laboratory, Kirtland AFB, NM, September 1982.
9. Terzaghi, K.; and Peck, R.; Soil Mechanics in Engineering Practice, John Wiley and Sons, New York, 1967.
10. Aki, K.; and Richards, P.; Quantitative Seismology: Theory and Methods, W.H. Freeman and Company, San Francisco, California, 1980.
11. Chernov, L., Wave Propagation in a Random Medium, McGraw-Hill, New York, 1960.



END

DATE  
FILMED

6-1988

DTIC